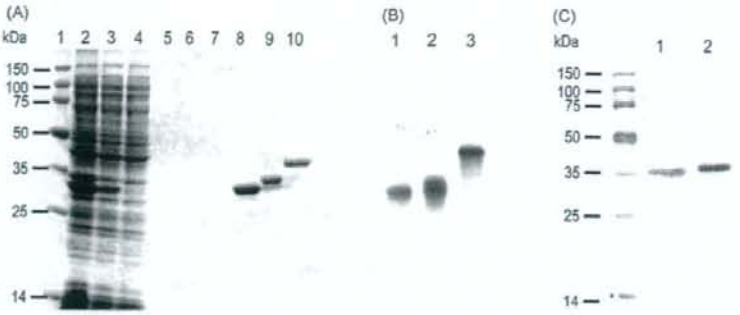

Fig. 3. Expression and purification of the recombinant EhSATs and detection of native EhSATs in the parasite lysate. (A) The *Escherichia coli* BL21 (DE3) strain was transformed with pET-EhSAT1, pET-EhSAT2, and pET-EhSAT3. The recombinant EhSAT1-3 protein was purified on a Ni^{2+}-NTA agarose column. Proteins at each step of purification were resolved on a 12.5% SDS-PAGE gel and stained with Coomassie Brilliant Blue. Lane 1, Molecular weight markers; lanes 2–4, the total lysate (2), supernatant fraction (3), or unbound fraction (4) of the IPTG-induced culture of the pET-EhSAT1-transformed cells; lanes 5–7, fractions eluted with 10, 20, and 50 mM imidazole, respectively; lanes 8–10, purified recombinant EhSAT1, EhSAT2, and EhSAT3, respectively, eluted with 200 mM imidazole. (B) Silver staining of the purified EhSAT1-3 (lanes 1–3, respectively). (C) Immunoblot analysis of the fractionated amebic lysate with anti-EhSAT1 and anti-EhSAT2 antibodies. A fraction eluted from a Mono Q anionic exchange chromatograph was electrophoresed, blotted, and reacted with 200× diluted anti-EhSAT1 (lane 1) or anti-EhSAT2 antibody (lane 2), followed by the reaction with the secondary antibody.

cytosolic SAT from watermelon, and plastid SAT from *A. thaliana* are shown to highlight important similarities and differences among SAT proteins from these organisms and between EhSAT isotypes (Fig. 1).

All the important residues implicated in the active site of the catalytic domain [31] are well conserved in EhSATs. For instance, the residues of Asp-114, Pro-115, Ala-116, Asp-179, and His-180 of EhSAT1, corresponding to Asp-92, Pro-93, Ala-94, Asp-157, and His-158, respectively, of *E. coli* SAT are well conserved. In contrast, there are also notable peculiarities of the amoebic SAT. First, *E. histolytica* SATs have a unique insertion between the coils 2 and 3 of the extended loop of LβH (a.a. 206–213 of EhSAT1-3, corresponding to between a.a. 183 and 184 of *E. coli* SAT). Interestingly, this insertion is also uniquely, other than in *Entamoeba*, present in *H. walsbyi*. Second, Thr-185 of *E. coli* SAT, which is responsible for the interaction with the carboxyl terminus of another subunit of a SAT trimer upon conformational changes caused by the L-cysteine attachment and subsequent in-sensitization of the enzyme to acetyl-CoA [32], is not conserved in amoebic SATs; this residue is substituted with Val or Ile in EhSAT1-3. Third, Ala-218 of *E. coli* SAT, which is involved in the hydrogen bonding with the carbonyl group of cofactor pantetheinyl moiety and the stabilization of CoA in the cleft between two subunits of the trimer [32], is substituted with Val-248 in all three amoebic SATs. Fourth, the amino acid residues around Met-256 of *E. coli* or Met-280 from watermelon have been implicated in the in-sensitivity to L-cysteine. For instance, the Gly-277 to Cys substitution caused in-sensitivity of watermelon SAT to L-cysteine. However, none of the residues in this region is conserved in EhSATs.

There are also isotype-specific features among EhSATs. In particular, EhSAT3 is significantly divergent. First, the amoeba-specific block insertion (a.a. 206–213) found in EhSAT1, EhSAT2, and two SATs from non-pathogenic *Entamoeba dispar* (data not shown) is not shared by EhSAT3. Second, EhSAT3 possesses a 26-a.a. carboxyl-terminal extension, similar to one in the cytosolic *A. thaliana* SAT, which is not shared by other amoebic SATs. Third, Ile-314 of *A. thaliana* SAT-p and in other organisms (*E. coli* or *H. influenza*), which is necessary for the complex formation with CS [33], is conserved in EhSAT1(Ile-305), it is not conserved in EhSAT2 and EhSAT3.

3.3. Phylogenetic analysis

Phylogenetic reconstruction was performed by NJ and MP programs using 35 SAT protein sequences from various organisms. The NJ tree (Fig. 2) demonstrates three major monophylic groups of SAT: the first group consisting of α-, β-, γ-, and δ-proteobacteria, cyanobacteria, *Bacteriodes*, and one archaeon organism, *Methanococcoides burtonii*, the second consisting of *Entamoeba* and *H. walsbyi*, and the third consisting of plants and a few bacteria belonging to α- and γ-proteobacteria. The high homology, the common amino acid insertion, and the phylogenetic relationship between SAT from *Entamoeba* and *H. walsbyi* suggest that *E. histolytica* most likely obtained a SAT gene from the ancestral organism of *H. walsbyi* by lateral gene transfer, similar to a number of metabolism enzymes [19,20,34]. Phylogenetic reconstruction using MP method also supports the above-mentioned conclusion (data not shown).

3.4. Expression and purification of recombinant EhSAT isotypes

The recombinant EhSATs were overproduced at the level of 20–25% of the soluble proteins in *E. coli* BL21 cells. 12% SDS-PAGE followed by Coomassie Brilliant Blue staining of the purified rEhSAT proteins showed that the rEhSAT1-3 was present as a single

Table 1
Kinetic parameters of EhSAT1, EhSAT2, and EhSAT3.

	L-Serine			Acetyl-CoA		
	K_m (mM)	V_{max} (μmol/min/mg)	k_{cat} (s)	K_m (mM)	V_{max} (μmol/min/mg)	k_{cat} (s)
Eh SAT1	0.12 ± 0.03	41.39 ± 1.43	25.52 ± 0.89	0.55 ± 0.20	95.10 ± 2.50	58.63 ± 2.67
Eh SAT2	0.09 ± 0.02	27.77 ± 1.57	17.31 ± 0.98	0.25 ± 0.02	23.42 ± 0.90	14.59 ± 0.56
Eh SAT3	0.10 ± 0.04	65.75 ± 3.15	43.83 ± 0.90	0.20 ± 0.07	176.83 ± 11.72	117.89 ± 7.81

Note: All reactions were performed as described under "Experimental procedures". All values are expressed as a mean ± S.E. of triplicates.

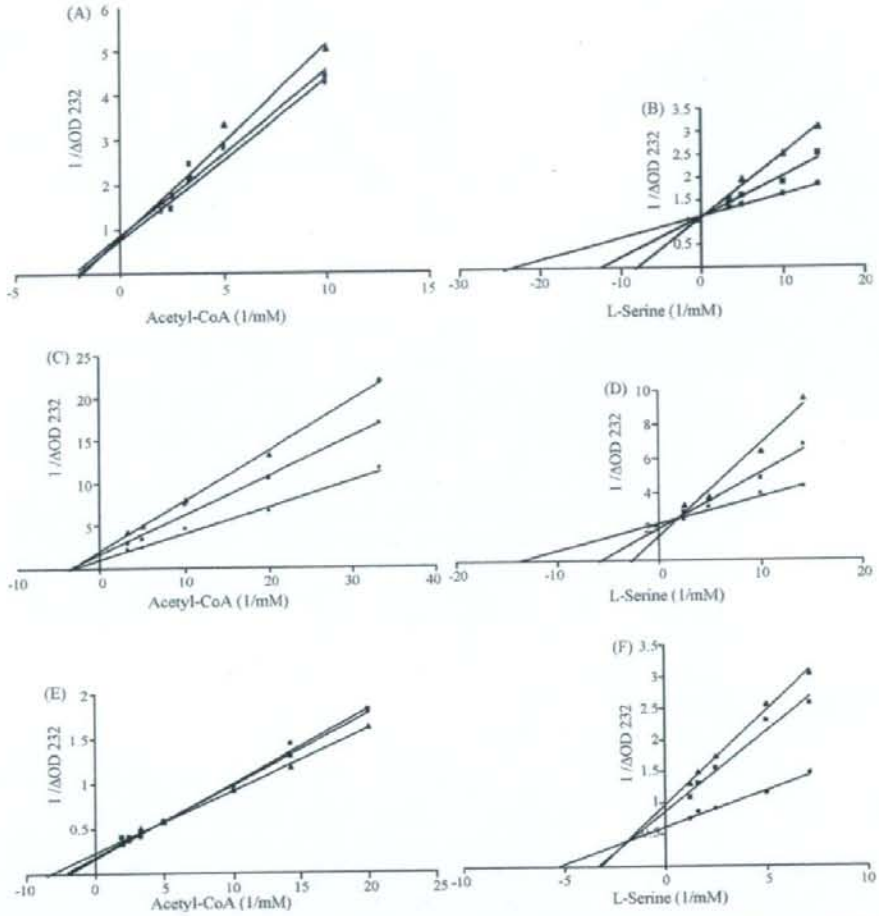

Fig. 4. Double-reciprocal plots of the recombinant EhSATs. The enzymatic activities of EhSAT1 (A and B), EhSAT2 (C and D), and EhSAT3 (E and F) were determined at various concentrations of acetyl-CoA (A, C, and E) and L-serine (B, D, and F) in the presence or absence of L-cysteine. Kinetic studies were performed by monitoring the decrease in A_{232} with a fixed concentration of 0.5 mM L-serine (A, C, and E) and 0.25 mM acetyl-CoA (B, D, and F). Data are shown in the mean of triplicate analyses. (A and B) Symbols are: ●, without L-cysteine; ■, in the presence of 5 μM L-cysteine; and ▲, 10 μM L-cysteine. (C and D) ●, without L-cysteine; ■, in the presence of 50 μM L-cysteine; and ▲, 100 μM L-cysteine. (E and F) ●, without L-cysteine; ■, in the presence of 0.5 mM L-cysteine; and ▲, 1 mM L-cysteine.

homogenous band corresponding to 37.0, 37.4, or 40.0 kDa, respectively, under reducing conditions (Fig. 3). The mobility of rEhSAT1-3 was consistent with the predicted size of the monomeric EhSAT proteins with an extra 2.6 kDa histidine tag added at the amino terminus. The purity of rEhSATs was estimated more than 95% as judged by densitometric scanning of the stained gel. EhSAT proteins were stable and retained their full activity when stored with 10–15% glycerol at −30 or −80 °C for at least 3 months. These purified EhSAT proteins showed no CS activity, suggesting that there is no interaction with *E. coli* CS (CysK and CysM) (data not shown).

3.5. Catalytic and regulatory properties of recombinant EhSATs

Since the purified recombinant EhSATs were free of bacterial CS, the catalytic and regulatory properties of these proteins could be examined without any influence of bacterial CS, which might otherwise potentially activates SAT. The kinetic parameters of rEhSAT1 determined in this study (Table 1) were consistent with those reported previously [17]. The K_m, the V_{max}, and the k_{cat} of three EhSAT proteins slightly varied, but were comparable.

The effects of L-cysteine on the activity of recombinant EhSATs were examined (Fig. 4A–F and Table 2). The inhibition of EhSAT by L-cysteine was isotype specific. The activity of EhSAT1 was inhibited by micromolar concentrations of L-cysteine. Double reciprocal plots in the presence or absence of 5 or 10 μM of L-cysteine, showed that the EhSAT1 activity was inhibited by L-cysteine in a competitive manner with L-serine, but no any significant inhibition was observed in case of acetyl-CoA in the presence of 0.25 mM of acetyl-CoA or 0.5 mM of L-serine (Fig. 4A and B and Table 2). EhSAT2 showed in-sensitivity to these concentrations (5 or 10 μM) of L-cysteine. Approximately 10-fold higher concentrations, i.e., 50–100 μM, of L-cysteine were needed to cause inhibition of EhSAT2 activity comparable to that of EhSAT1. Double reciprocal plots showed that the EhSAT2 activity was inhibited by L-cysteine

Table 2
Inhibition constants (K_i) of recombinant *E. histolytica* SATs by L-cysteine.

	K_i (μM)		
	L-Serine	Acetyl-CoA	Sensitivity
EhSAT1	4.7 ([b]competitive)	[a]–	Sensitive
EhSAT2	27.79 ([b]competitive)	94.7 ([b]non-competitive)	Intermediate
EhSAT3	460 ([b]mix)	[a]–	Insensitive

The enzymatic activities were determined in vitro as described under section 2. To determine the K_i value for L-serine or acetyl-CoA, the constant concentration of acetyl-CoA (0.25 mM) or L-serine (0.5 mM) was used. All values are expressed as a mean ± S.E. of triplicates.

[a] No inhibition by L-cysteine.

[b] The mode of inhibition is shown in parenthesis.

Table 3
Inhibition of EhSATs by structurally related compounds.

Compounds	Concentrations (mM)	Inhibition (%)		
		EhSAT1	EhSAT2	EhSAT3
L-Cysteine	0.03	97.3	<0.5	<0.5
L-Cysteine	0.5	95.4	75.3	<0.5
L-Cysteine	1	98.5	ND	37.8
L-Cystine	0.03	3.6	0.9	7.9
D-Cysteine	0.5	2.2	3.9	4.8
DL-Homocysteine	0.5	7.7	0.9	8.7
DL-Homoserine	0.5	7.7	8.8	5.5
N-Acetyl-L-cysteine	1	25	13.3	27.8
N-Acetyl-L-serine	0.5	11.8	4.9	7.9
Glutathione (oxidized)	0.5	1.3	0.9	19.9
Glutathione (reduced)	0.5	ND	10.3	10.7

ND, Not determined.

in a competitive manner with L-serine and in a non-competitive manner with acetyl-CoA (Fig. 4C and D and Table 2). The K_i value of EhSAT2 by L-cysteine was about 6-fold higher than that of EhSAT1.

In contrast, EhSAT3 was totally in-sensitive to L-cysteine at the concentrations that abolished EhSAT1 and EhSAT2 activity, and very high concentrations of L-cysteine (0.5 or 1 mM) were required to inhibit EhSAT3 activity. At these L-cysteine concentrations, the pattern of inhibition was in a mixed manner with L-serine, but no inhibition was seen for acetyl-CoA (Fig. 4E and F and Table 2). The K_i value of EhSAT3 by L-cysteine was 98 or 18-fold higher than that of EhSAT1 or EhSAT2, respectively.

3.6. Inhibition of EhSAT activity by compounds structurally related to L-cysteine

L-Cysteine showed significant inhibition of EhSAT1 at 30 μM (97%), when 0.5 mM L-serine and 0.2 mM of acetyl-CoA were used. Under the identical conditions, only weak inhibition was observed at 30 μM of L-cystine (<4%), which is contradictory to our previous report [17], but in accordance with other reports on SAT from plants and bacteria. This contradiction might be due to the new expression protocol and the far better purity of EhSAT1 obtained in the present study. Other compounds showed no inhibition against EhSAT1 except for N-acetyl-L-serine and N-acetyl-L-cysteine (Table 3). EhSAT2 was inhibited with 0.5 mM L-cysteine by 75%, while N-acetyl-L-cysteine and reduced glutathione showed marginal inhibition. Inhibition of EhSAT3 by 1 mM L-cysteine, 1 mM N-acetyl-L-cysteine, or 0.5 mM oxidized glutathione was significant, while other compounds showed no inhibition.

3.7. Effect of L-serine on the sensitivity of EhSATs to L-cysteine inhibition

We also directly tested whether the three SAT enzymes are differentially inhibited by L-cysteine in the presence of the physiological L-serine concentrations. L-Cysteine at the concentrations of 5–500 μM remarkably inhibited EhSATs in the presence of 0.5 mM of L-serine (Fig. 4 and Table 1). In contrast, in the presence of 3 mM of L-serine, which was equivalent to the concentration in the axenically cultured trophozoites (3.2 mM), [35], L-cysteine at the same concentrations showed much less inhibition (Fig. 5). Thus, not only the L-cysteine, but also L-serine (and acetyl-CoA, data not shown) concentration affects the EhSAT activity. At known L-cysteine and L-serine concentrations in axenically cultured trophozoites (0.3 and 3.2 mM, respectively), EhSAT1 and EhSAT2 activity was inhibited by approximately 90 or 20%, respectively, while EhSAT3 activity remained fully active. These data suggest that the activity of EhSAT1 and EhSAT2 is modulated under the *in vivo* conditions, where the L-serine and L-cysteine concentrations likely fluctuate.

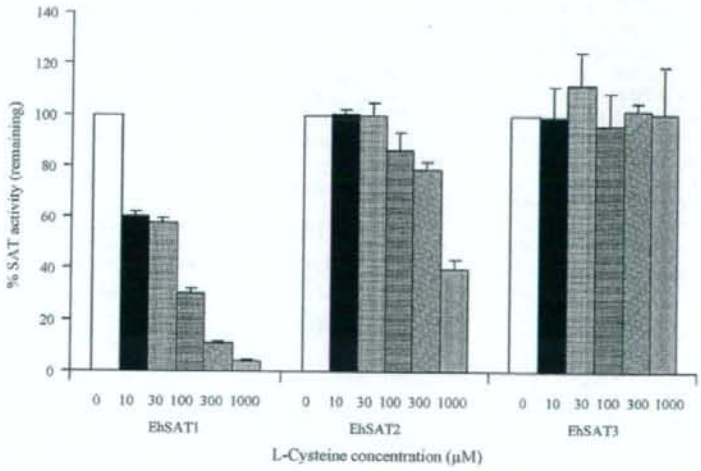

Fig. 5. Effects of various L-cysteine concentrations on the activity of EhSAT isotypes in the presence of physiological concentrations of L-serine (3 mM). The SAT activity is shown in percentage relative to that of the individual SAT isotype measured in the absence of L-cysteine.

3.8. Cellular distribution of EhSATs in E. histolytica trophozoites

We examined cellular distribution of three isotypes of EhSAT in the HM1 reference strain. The immunofluorescence imaging using antiserum raised against the corresponding recombinant protein showed that all the three isotypes are distributed to the cytosol (data not shown). We also verified the expression of EhSATs by immunoblots. The lysate was produced by freezing and thawing followed by sonication and centrifugation at 100,000 × *g* centrifugation (at 4 °C for 1 h). Immunoblots showed that EhSAT1 and 2 were fractionated to the soluble fraction (for clarity of immunoblots, the immunolots using a fraction which was obtained by further separation on anionic exchange chromatography is shown in Fig. 3C).

4. Discussion

In the present study, we have reported for the first time that *E. histolytica* possesses multiple isotypes of SAT with distinct properties. Although the presence of sulfur assimilatory cysteine biosynthetic pathway has been well documented in this parasite [18,36], and the feedback-inhibition of EhSAT1 by L-cysteine was previously reported [17], the existence of apparently redundant systems, consisting of multiple isoenzymes catalyzing identical reactions (i.e., EhSAT1-3 as well as CS isotypes, EhCS1-3, unpublished [18,20,37]), strengthen biological significance of regulation of L-cysteine synthesis in this organism. Although their subcellular localization has not been demonstrated, the lack of the organelle targeting signals, as seen in organelle-located SAT from plants [26,27], in EhSAT1-3 and the lack of the typical mitochondria and plastids in this organism [17] support the premise that the all three amoebic SAT isotypes are cytosolic. Immunofluorescence and cellular fractionation studies also suggest that all the three SAT isotypes are located to the cytosol. Isoform-dependent feedback-inhibition of SAT, often compartmentalized to the cytosol, chloroplast, and mitochondria, by L-cysteine was previously demonstrated in plants [8]. Thus, the present work is the first report showing the presence of multiple cytosolic SAT isoforms with distinct features.

The three SAT isotypes from *E. histolytica* showed high, intermediate, and low sensitivity to inhibition by L-cysteine. The sensitivity of EhSATs to the cysteine inhibition varies in two orders of magnitude (the K_i value of EhSAT1-3 was 4.7, 28, and 460 μM, respectively, Table 2). We have also shown that L-serine at the physiological concentrations modulates the sensitivity of EhSATs to L-cysteine. Furthermore, the modulation of the L-cysteine sensitivity by L-serine is isotype specific. Under the reported intracellular cysteine concentrations of axenically cultured trophozoites (0.3 mM), [35], the activity of EhSAT1 is predicted to be totally suppressed in this parasite. Alternatively, EhSAT1 may be compartmentalized to a confined region of the cytosol where the L-cysteine concentration is low. Although the intracellular L-serine and L-cysteine concentrations in the amoeba in the human remain unknown, it is conceivable that they vary under different conditions of its life cycle and infection, e.g., in the human colonic lumen and invaded tissues. Thus, the redundancy of CS/SAT and cysteine biosynthesis may be necessary to ensure replenishment of L-cysteine under various physiological and pathological conditions where the amino acid availability fluctuates.

In bacteria, L-cysteine at micromolar concentrations inhibits SAT activity and OAS acts not only as a substrate but also as an inducer of Cys regulon [5]. Since EhSAT3 is virtually insensitive to L-cysteine inhibition, L-cysteine production is not regulated unless EhSAT3 activity is regulated by other unidentified mechanisms including compartmentalization. Although roles of OAS remain totally promiscuous in this organism, it is plausible if OAS also regulates expression of genes involved in L-cysteine biosynthesis. It has been known in bacteria [5] under the L-cysteine-limited conditions, SATs do not only provide OAS for the replenishment of L-cysteine through desensitization of L-cysteine inhibition, but also induces the expression of genes involved in L-cysteine biosynthesis [38].

The previous transcriptome analysis [37] suggested all three EhSAT genes are expressed in axenic cultures; EhSAT1 and EhSAT3 are well expressed, while EhSAT2 is 10–40-fold less expressed than the other two isoforms. It was also demonstrated that expression of *EhSAT1* or *EhSAT2* gene was 3.4–6.0-fold downregulated or 4.1–8.7-fold upregulated, respectively, during the intestinal infection, whereas the expression of *EhSAT3* gene remained unchanged (only 1.5–1.6-fold repression). These data suggest that individual *EhSAT* genes are under coordinated regulation of expression under different physiological conditions and also that EhSAT2 might have a specific role in intestinal colonization.

Structural understanding of the in-sensitivity of EhSAT3 to the L-cysteine inhibition is underway. The carboxyl-terminal extension unique to EhSAT3 is one of the obvious points of interest involved in protein–protein interactions. The carboxyl-terminal region has also been implicated in the CS complex formation, as the 10–25 a.a. carboxyl-terminal truncation caused dissociation of SAT from CS in *E. coli* [39,40]. Further investigation of truncation and mutation by site-directed and PCR-based random mutagenesis, as shown in bacterial and plant SATs [39,41], is necessary. Finally, since the sulfur assimilatory cysteine biosynthetic pathway is absent from human, it should provide a suitable target for the rational development of new chemotherapeutics against amoebiasis. Recent demonstration of inhibition of *E. histolytica* trophozoites proliferation by compounds devised *in silico* by docking to *E. coli* SAT (NCI 128884, 29607, and 653543) [42] reinforced the premise. Therefore, the detailed study of its components, as shown in the present study, is important to validate the suitability of the target.

Acknowledgements

We thank Dan Sato, Afzal Husain, and all other members of our laboratory for the technical assistance and valuable discussions. This work was supported by a fellowship from the Japan Society for the Promotion of Science to S.H. (P06240), Grant-in-Aids for Scientific Research from the Ministry of Education, Culture, Sports, Science and Technology of Japan to V.A. (19790303) and T.N. (18GS0314, 18050006, 18073001), a grant for research on emerging and re-emerging infectious diseases from the Ministry of Health, Labour and Welfare of Japan to T.N., and a grant for research to promote the development of anti-AIDS pharmaceuticals from the Japan Health Sciences Foundation to T.N.

References

[1] Saito K. Biosynthesis of cysteine. In: Singh B, editor. Plant amino acids: biochemistry and biotechnology. New York: Marcel Dekker; 1998. p. 267–91.
[2] Leustek T. Molecular genetics of sulfate assimilation in plants. Physiol Plant 1996;97:411–9.
[3] Hell R. Molecular physiology of plant sulfur metabolism. Planta 1997;202:138–48.
[4] Brunold C, Rennenberg H. Regulation of sulfur metabolism in plants: first molecular approaches. Prog Bot 1997;58:164–86.
[5] Kredich NM, Tomkins GM. The enzymic synthesis of L-cysteine in *Escherichia coli* and *Salmonella typhimurium*. J Biol Chem 1966;241:4955–65.
[6] Hesse H, Nikiforova V, Gakière B, Hoefgen R. Molecular analysis and control of cysteine biosynthesis: integration of nitrogen and sulphur metabolism. J Exp Bot 2004;55:1283–92.
[7] Saito K, Yokoyama H, Noji M, Murakoshi I. Molecular cloning and characterization of a plant serine acetyltransferase playing a regulatory role in cysteine biosynthesis from watermelon. J Biol Chem 1995;270:16321–6.
[8] Noji M, Inoue K, Kimura N, Gouda A, Saito K. Isoform-dependent differences in feedback regulation and subcellular localization of serine acetyltrans-

ferase involved in cysteine biosynthesis from *Arabidopsis thaliana*. J Biol Chem 1998;273:32739–45.
[9] Howarth JR, Roberts MA, Wray JL. Cysteine biosynthesis in higher plants: a new member of the *Arabidopsis thaliana* serine acetyltransferase small gene-family obtained by functional complementation of an *Escherichia coli* cysteine auxotroph. Biochem Biophys Acta 1997;1350:123–7.
[10] Murillo M, Foglia R, Diller A, Lee S, Leustek T. Serine acetyltransferase from *Arabidopsis thaliana* can functionally complement the cysteine requirement of a *cysE* mutant strain of *Escherichia coli*. Cell Mol Biol Res 1995;41:425–33.
[11] Ruffet ML, Lebron M, Droux M, Douce R. Subcellular distribution of serine acetyltransferase from *Pisum sativum* and characterization of an *Arabidopsis thaliana* putative cytosolic isoform. Eur J Biochem 1995;227:500–9.
[12] Bogdanova N, Bork C, Hell R. Cysteine biosynthesis in plants: isolation and functional identification of a cDNA encoding a serine acetyltransferase from *Arabidopsis thaliana*. FEBS Lett 1995;358:43–7.
[13] Hell R, Bogdanova N. Characterization of a full-length cDNA encoding serine acetyltransferase from *Arabidopsis thaliana*. Plant Physiol 1995;109:1498.
[14] Roberts MA, Wray JL. Cloning and characterization of an *Arabidopsis thaliana* cDNA clone encoding an organellar isoform of serine acetyltransferase. Plant Mol Biol 1996;30:1041–9.
[15] World Health Organization/Pan American Health Organization. Report of a consultation of experts on amoebiasis. Weekly Epidemiol Rep 1997;72:97–9.
[16] Nozaki T, Asai T, Kobayashi S, et al. Molecular cloning and characterization of the genes encoding two isoforms of cysteine synthase in the enteric protozoan parasite, *Entamoeba histolytica*. Mol Biochem Parasitol 1998;97:33–44.
[17] Nozaki T, Asai T, Sanchez LB, Kobayashi S, Nakazawa M, Takeuchi T. Characterization of the gene encoding serine acetyltransferase, a regulated enzyme of cysteine biosynthesis from the protist parasites *Entamoeba histolytica* and *Entamoeba dispar*. Regulation and possible function of the cysteine biosynthetic pathway in *Entamoeba*. J Biol Chem 1999;274:32445–52.
[18] Nozaki T, Ali V, Tokoro M. Sulfur-containing amino acid metabolism in parasitic protozoa. Adv Parasitol 2005;60:1–99.
[19] Loftus B, Anderson I, Davies R, et al. The genome of the protist parasite *Entamoeba histolytica*. Nature 2005;433:865–8.
[20] Clark CG, Alsmark UC, Tazreiter M, et al. Structure and content of the *Entamoeba histolytica* genome. Adv Parasitol 2007;65:51–190.
[21] Nozaki T, Tokoro M, Imada M, et al. Cloning and biochemical characterization of genes encoding two isozymes of cysteine synthase from *Entamoeba dispar*. Mol Biochem Parasitol 2000;107:129–33.
[22] Diamond LS, Harlow DR, Cunnick CC. A new medium for the axenic cultivation of *Entamoeba histolytica* and other *Entamoeba*. Trans R Soc Trop Med Hyg 1978;72:431–2.
[23] Clark CG, Diamond LS. Methods for cultivation of luminal parasitic protists of clinical importance. Clin Microbiol Rev 2002;15:329–41.
[24] Sambrook J, Russell DW. Molecular cloning: a laboratory manual. 2nd ed. Cold Spring Harbor: Cold Spring Harbor Laboratory Press; 2001.
[25] Bradford MM. A rapid and sensitive method for the quantitation of microgram quantities of protein utilizing the principle of protein–dye binding. Anal Biochem 1976;72:248–54.
[26] Baecker PA, Wedding RT. Purification of serine acetyltransferase, a component of a multienzyme complex, by immunoadsorption and selective dissociation of the complex. Anal Biochem 1980;102:16–21.
[27] Nakamura K, Hayama A, Masada M, Fukushima K, Tamura G. Purification and some properties of plant serine acetyltransferase. Plant Cell Physiol 1988;29:689–93.
[28] Saito K, Miura N, Yamazaki M, Hirano H, Murakoshi I. Molecular cloning and bacterial expression of cDNA encoding a plant cysteine synthase. Proc Natl Acad Sci USA 1992;89:8078–82.
[29] Thompson JD, Higgins DG, Gibson TJ. CLUSTAL W: improving the sensitivity of progressive multiple sequence alignment through sequence weighting, position-specific gap penalties and weight matrix choice. Nucleic Acids Res 1999;22:4673–80.
[30] Kumar S, Tamura K, Jakobsen IB, Nei M. MEGA2: molecular evolutionary genetics analysis software. Bioinformatics 2001;17:1244–5.
[31] Pye VE, Tingey AP, Robson RL, Moody PC. The structure and mechanism of serine acetyltransferase from *Escherichia coli*. J Biol Chem 2004;279:40729–36.
[32] Olsen LR, Huang B, Vetting MW, Roderick SL. Structure of serine acetyltransferase in complexes with CoA and its cysteine feedback inhibitor. Biochemistry 2004;43:6013–9.
[33] Francois JA, Kumaran S, Jez JM. Structural basis for interaction of *O*-acetylserine sulfhydrylase and serine acetyltransferase in the *Arabidopsis* cysteine synthase complex. Plant Cell 2006;18:3647–55.
[34] Anderson I, Loftus B. *Entamoeba histolytica*: observations on metabolism based on the genome. Exp Parasitol 2005;110:173–7.
[35] Bakker-Grunwald T, Martin JB, Klein G. Characterizing of glycogen and amino acid pool of *Entamoeba histolytica* by 13C-NMR spectroscopy. J Euk Microbiol 1995;42:346–9.
[36] Ali V, Nozaki T. Current therapeutics, their problems, and sulfur-containing amino acid metabolism as a novel target against infections by "amitochondriate" protozoan parasites. Clin Microbiol Rev 2007;20:164–87.
[37] Gilchrist CA, Houpt E, Trapaidze N, et al. Impact of intestinal colonization and invasion on the *Entamoeba histolytica* transcriptome. Mol Biochem Parasitol 2006;147:163–76.
[38] Kredich NM. *Escherichia coli* and *Salmonella*. In: Curtiss R, Ingraham JL, Lin ECC, Low KB, Magasanik B, Reznikoff WS, Riley M, Schaechter M, Umbarger HE, editors. Cellular and molecular biology. American Society for Microbiology Press; 1996. p. 514–27.
[39] Mino K, Yamanoue T, Sakiyama T, Eisaki N, Matsuyama A, Nakanishi K. Purification and characterization of serine acetyltransferase from *Escherichia coli* partially truncated at the C-terminal region. Biosci Biotechnol Biochem 1999;63:168–79.
[40] Mino K, Yamanoue T, Sakiyama T, Eisaki N, Matsuyama A, Nakanishi K. Effects of bienzyme complex formation of cysteine synthetase from *Escherichia coli* on some properties and kinetics. Biosci Biotechnol Biochem 2000;64:1628–40.
[41] Denk D, Bock A. L-Cysteine biosynthesis in *Escherichia coli*: nucleotide sequence and expression of the serine acetyltransferase (cysE) gene from the wild-type and a cysteine-excreting mutant. J Gen Microbiol 1987;133:515–25.
[42] Agarwal SM, Jain R, Bhattacharya A, Azam A. Inhibitors of *Escherichia coli* serine acetyltransferase block proliferation of *Entamoeba histolytica* trophozoites. Int J Parasitol 2008;38:137–41.

Acta Crystallographica Section F
Structural Biology and Crystallization Communications
ISSN 1744-3091

Crystallization and preliminary X-ray analysis of L-methionine γ-lyase 1 from *Entamoeba histolytica*

Dan Sato,[a,b,c] Tsuyoshi Karaki,[d] Akira Shimizu,[d] Kaeko Kamei,[d] Shigeharu Harada[d]* and Tomoyoshi Nozaki[c,e]

[a]Institute for Advanced Biosciences, Keio University, 246-2 Mizukami, Kakuganji, Tsuruoka, Yamagata 997-0052, Japan, [b]Center for Integrated Medical Research, School of Medicine, Keio University, 35 Shinanomachi, Shinjuku-ku, Tokyo 160-8582, Japan, [c]Department of Parasitology, Gunma University Graduate School of Medicine, 3-39-22 Showa-machi, Maebashi, Gunma 371-8511, Japan, [d]Graduate School of Science and Technology, Department of Applied Biology, Kyoto Institute of Technology, Sakyo-ku, Kyoto 606-8585, Japan, and [e]Department of Parasitology, National Institute of Infectious Diseases, 1-23-1 Toyama, Shinjuku-ku, Tokyo 162-8640, Japan

Correspondence e-mail: harada@kit.ac.jp

Received 19 April 2008
Accepted 20 June 2008

L-Methionine γ-lyase (MGL) is a pyridoxal phosphate-dependent enzyme that is involved in the degradation of sulfur-containing amino acids. MGL is an attractive drug target against amoebiasis because the mammalian host of its causative agent *Entamoeba histolytica* lacks MGL. For the development of anti-amoebic agents based on the structure of MGL, one of two MGL isoenzymes (EhMGL1) was crystallized in the monoclinic space group $P2_1$, with unit-cell parameters $a = 99.12$, $b = 85.38$, $c = 115.37$ Å, $\beta = 101.82°$. The crystals diffract to beyond 2.0 Å resolution. The presence of a tetramer in the asymmetric unit (4 × 42.4 kDa) gives a Matthews coefficient of 2.8 Å^3 Da^{-1} and a solvent content of 56%. The structure was solved by the molecular-replacement method and structure refinement is now in progress.

1. Introduction

Amoebiasis, which is caused by infection with the enteric protist *Entamoeba histolytica*, is the second largest parasitic disease after malaria; it affects over 50 million people and results in 70 000 deaths annually (World Health Organization, 1998). Its major clinical manifestations are amoebic dysentery and extraintestinal abscesses (Stanley, 2003).

The sulfur-containing amino-acid metabolism of *E. histolytica* has a number of unique features (Nozaki *et al.*, 2005; Ali & Nozaki, 2007). For example, *E. histolytica* lacks the transsulfuration pathway and thus is unable to convert methionine to cysteine and *vice versa*. Instead, it possesses L-methionine γ-lyase (MGL; EC 4.4.1.11), which is involved in the degradation of sulfur-containing amino acids (Tokoro *et al.*, 2003; Sato *et al.*, 2008). MGL contains pyridoxal 5′-phosphate (PLP) as a cofactor and has been categorized as belonging to the γ-family of PLP-dependent enzymes (Alexander *et al.*, 1994). MGL catalyzes α,γ- or α,β-elimination of sulfur-containing amino acids and produces ammonia, α-keto acids and volatile thiols such as hydrogen sulfide or methanethiol (Tanaka *et al.*, 1985). It also catalyzes β- or γ-replacement of cysteine, *S*-substituted cysteine, methionine and related compounds (Tanaka *et al.*, 1985). MGL is only present in a limited range of bacteria, protozoa and plants (Nakayama *et al.*, 1984; Kreis & Hession, 1973; Yoshimura *et al.*, 2000; Dias & Weimer, 1998; Manukhov *et al.*, 2005; Goyer *et al.*, 2007; Coombs & Mottram, 2001; Nozaki *et al.*, 2005; Rebeille *et al.*, 2006). Crystal structures have been reported for MGLs from *Pseudomonas putida* (Motoshima *et al.*, 2000; Sridhar *et al.*, 2000), *Trichomonas vaginalis* (PDB code 1e5f; G. Goodall, J. C. Mottram, G. H. Coombs & A. J. Lapthorn, unpublished work) and *Citrobacter freundii* (Mamaeva *et al.*, 2005; Nikulin *et al.*, 2008).

MGLs from parasitic protozoa are unique in that they exist as two isoenzymes with distinct substrate specificities (*e.g.* EhMGL1 and EhMGL12 in *E. histolytica*; 69% amino-acid sequence identity; Tokoro *et al.*, 2003; Sato *et al.*, 2008). A previous study demonstrated that EhMGL1, but not EhMGL2, predominantly degrades methionine and cysteine (Sato *et al.*, 2008). In contrast, trifluoromethionine (TFM), the halogenated analogue of methionine, which exhibits toxicity by being degraded by MGL in *Porphyromonas gingivalis*,

T. vaginalis and *E. histolytica* (Yoshimura *et al.*, 2002; Coombs & Mottram, 2001; Tokoro *et al.*, 2003), was almost exclusively degraded by EhMGL2. We also showed that the K_m of EhMGL1 towards TFM was ninefold lower than that of EhMGL2, while the k_{cat} of EhMGL2 was 22-fold higher than that of EhMGL1 (Sato *et al.*, 2008), indicating that the catalytic action of MGLs towards TFM might be different. For structure-based design of TFM derivatives, comparison of the tertiary structures of the two EhMGL isotypes should be helpful. We have previously crystallized ligand-free EhMGL2 (Sato *et al.*, 2006) and determined its X-ray structure as well as those of structures of complexes with substrates and inhibitors (unpublished results). In the present study, we describe the bacterial expression, purification, crystallization and preliminary X-ray diffraction studies of EhMGL1.

2. Materials and methods

2.1. Overexpression and purification of recombinant MGL1

When we attempted to express the *EhMGL1* gene (AB094499) in a bacterial expression system (pGEX-6P-1 vector; GE Healthcare Biosciences) as an amino-terminal glutathione *S*-transferase (GST) fusion protein, a fraction of protein (~20%) was produced as a truncated form starting from Gly46 (Sato *et al.*, 2008). This truncation was caused by an inadvertent translation initiation at Met45 which was likely to be a consequence of the similarity of the nucleotide sequence upstream of Met45 to the Shine–Dalgarno sequence. We therefore mutated five nucleotides in this region, which did not cause amino-acid substitution (Sato *et al.*, 2008). This genetically engineered EhMGL1 construct allowed us to successfully express and purify EhMGL1 protein without truncation. For large-scale preparation, this plasmid was introduced into the *Escherichia coli* BL21 Star (DE3) strain (Invitrogen) and the transformant was grown in 2 l M9 minimal medium (Sambrook *et al.*, 1989) supplemented with 1 m*M* $MgSO_4$, 0.1 m*M* $CaCl_2$, 3.3 μM $FeCl_3$, 59 μM thiamine–HCl, 82 μM biotin, 20 μM PLP and 50 $\mu g\ ml^{-1}$ ampicillin at 310 K. The medium was prepared with commercially available mineral water to supply trace elements. The induction of expression, affinity purification and on-column digestion of the GST-EhMGL1 fusion protein were carried out as described previously for EhMGL2 (Sato *et al.*, 2006). The fraction containing GST-removed EhMGL1 was eluted from a GSTrap HP column (1.6 × 2.5 cm; GE Healthcare Biosciences) with 50 m*M* HEPES–NaOH pH 7.5, 150 m*M* NaCl and 20 μM PLP and concentrated to 1–2 ml with Amicon Ultra-4 Ultracel-10K. EhMGL1 was further purified by size-exclusion chromatography on a HiPrep 16/60 Sephacryl S-300 column (16 × 60 cm; GE Healthcare Biosciences) equilibrated with 50 m*M* sodium phosphate pH 7.2 containing 150 m*M* NaCl and 20 μM PLP. EhMGL1 was eluted as a tetramer as previously described (Tokoro *et al.*, 2003). The purified EhMGL1 contained ten extra amino-acid residues (GPLGSPEFPG) at the amino-terminus derived from the linker peptide between GST and EhMGL1. The fractions containing the recombinant EhMGL1 were dialyzed against 10 m*M* HEPES–NaOH pH 7.4 and concentrated using an Amicon Ultra-4 Ultracel-50K to ~20 $mg\ ml^{-1}$. About 10 mg purified EhMGL1 was produced from 2 l culture. The purity was estimated to be >95% pure by densitometric quantitation of the corresponding band on SDS–PAGE (Fig. 1, lane 4) and the retained activity was comparable to the previous study (Sato *et al.*, 2008).

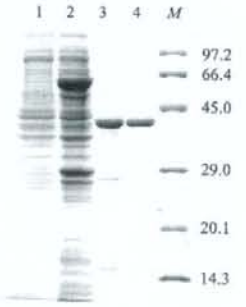

Figure 1
A 12% SDS–PAGE gel stained with Coomassie Brilliant Blue showing the apparent homogeneity of the purified EhMGL1. Lane 1, *E. coli* soluble extract before IPTG induction; lane 2, *E. coli* soluble extract after IPTG induction; lane 3, an eluate from a GSTrap HP column after digestion with PreScission Protease; lane 4, the purified EhMGL1 after size-exclusion chromatography using a HiPrep16/60 Sephacryl S-300 column; lane *M*, molecular-weight markers (kDa).

2.2. Crystallization and X-ray diffraction data collection

Crystallization conditions were screened at 277 and 293 K by the sitting-drop vapour-diffusion method in 96-well CrystalClear Strips (Hampton Research). A 0.5 µl droplet containing about 20 $mg\ ml^{-1}$ EhMGL1 dissolved in 10 m*M* HEPES–NaOH pH 7.4 was mixed with an equal volume of reservoir solution and the droplet was allowed to equilibrate against 100 µl reservoir solution. In the initial screening experiment, Crystal Screen (Jancarik & Kim, 1991), Crystal Screen II (Hampton Research) and Wizard Screens I and II (Emerald Biostructures) were used as reservoir solutions. Of the 194 conditions used, reagents containing ammonium sulfate as a precipitant gave thin plate-shaped crystals at 277 K. Conditions were further optimized at 277 K by varying the concentration of ammonium sulfate and the buffer pH. The effects of additives were also examined using Additive Screen kits from Hampton Research. The best crystals grew at 277 K from reservoir solution containing 1.8 *M* ammonium sulfate, 0.1 *M* cacodylate buffer pH 6.2, 0.1 *M* lithium citrate and 0.01 *M* betaine.

For X-ray diffraction experiments at 100 K, a crystal mounted in a nylon loop was transferred into and briefly soaked in a solution containing 2.2 *M* ammonium sulfate, 0.1 *M* cacodylate buffer pH 6.2, 0.1 *M* lithium citrate, 0.01 *M* betaine and 20%(*w*/*v*) glycerol and then frozen by rapidly submerging it in liquid nitrogen. X-ray diffraction data were collected using the rotation method on the BL5A beamline of Photon Factory (Tsukuba, Japan) at a wavelength of 1.000 Å using

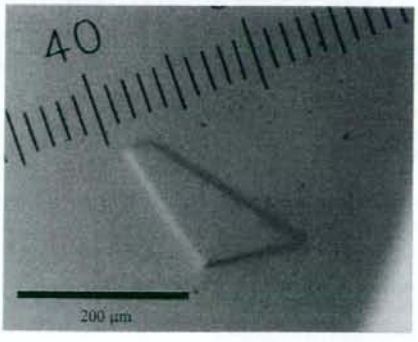

Figure 2
A typical crystal of EhMGL1.

Table 1
Data-collection and processing statistics.

Values in parentheses are for the highest resolution shell.

Wavelength (Å)	1.000
Space group	$P2_1$
Unit-cell parameters	
a (Å)	99.12
b (Å)	85.38
c (Å)	115.37
β (°)	101.82
Solvent content† (%)	56
Resolution range (Å)	50.0–1.93 (2.00–1.93)
No. of reflections	491182
Unique reflections	140502
Completeness (%)	96.3 (87.0)
R_{merge}‡ (%)	7.2 (39.1)
$I/\sigma(I)$	8.4 (2.57)

† Assuming the presence of four molecules in the asymmetric unit. ‡ $R_{merge} = \sum_{hkl}\sum_i |I_i(hkl) - \langle I(hkl)\rangle| / \sum_{hkl}\sum_i I_i(hkl)$.

a CCD ADSC Quantum 315 detector. A total of 180 frames were recorded with an oscillation angle of 1.0°, an exposure time of 5.0 s per frame and a crystal-to-detector distance of 213 mm. Data were processed and scaled with *HKL*-2000 and *SCALEPACK* (Otwinowski & Minor, 1997).

3. Results and discussion

Of the 194 crystallization conditions screened using commercially available screening kits, reagents containing ammonium sulfate gave thin plate-shaped crystals. After optimization of the pH, the concentration of ammonium sulfate and additives, crystals grew to typical dimensions of 0.02 × 0.3 × 0.4 mm (Fig. 2) in 5 d under the conditions 1.8 *M* ammonium sulfate, 0.1 *M* cacodylate buffer pH 6.2, 0.1 *M* lithium citrate and 0.01 *M* betaine at 277 K. Diffraction patterns were recorded as 180 frames at 100 K using one crystal. Analysis of the symmetry and systematic absences in the recorded diffraction patterns indicated that the crystals belonged to the monoclinic space group $P2_1$, with unit-cell parameters a = 99.12, b = 85.38, c = 115.37 Å, β = 101.82°. Assuming the presence of four EhMGL1 molecules (4 × 42.4 kDa) in the asymmetric unit, the V_M value was calculated to be 2.8 Å^3 Da^{-1} with an estimated solvent content of 56%; these values are within the range commonly observed for protein crystals (Matthews, 1968). A total of 491 182 observed reflections were merged to 140 502 unique reflections in the 50.0–1.93 Å resolution range. The data-collection and processing statistics are summarized in Table 1.

An attempt to solve the structure using the molecular-replacement method with the *MOLREP* program (Navaza, 1994) as implemented within the *CCP*4 package (Collaborative Computational Project, Number 4, 1994) was carried out using the refined coordinates of EhMGL2 (unpublished results; 69% sequence identity to EhMGL1). A promising solution with a homotetramer structure was obtained (correlation coefficient and R factor of 0.557 and 51.3%, respectively) and the model was subsequently subjected to rigid-body refinement, giving an R factor of 46.8%. Amino-acid residues of the initial homotetramer model that differ from those of the search model were replaced with Ala. Using the molecular-replacement solution, refinement of the tetramer structure of EhMGL1 is in progress. In parallel with the refinement, we are now trying to prepare crystals of EhMGL1 complexed with substrate analogues and inhibitors.

We are grateful to staff members at the BL5A beamline at Photon Factory for their help with X-ray diffraction data collection. This work was supported by a Grant-in-Aid for Scientific Research from the Ministry of Education, Culture, Sports, Science and Technology of Japan to DS (20590429) and TN (18050006, 18073001) and a grant for research to promote the development of anti-AIDS pharmaceuticals from the Japan Health Sciences Foundation to TN.

References

Alexander, F. W., Sandmeier, E., Mehta, P. K. & Christen, P. (1994). *Eur. J. Biochem.* **219**, 953–960.
Ali, V. & Nozaki, T. (2007). *Clin. Microbiol. Rev.* **20**, 164–187.
Collaborative Computational Project, Number 4 (1994). *Acta Cryst.* D**50**, 760–763.
Coombs, G. H. & Mottram, J. C. (2001). *Antimicrob. Agents Chemother.* **45**, 1743–1745.
Dias, B. & Weimer, B. (1998). *Appl. Environ. Microbiol.* **64**, 3327–3331.
Goyer, A., Collakova, E., Shachar-Hill, Y. & Hanson, A. D. (2007). *Plant Cell Physiol.* **48**, 232–242.
Jancarik, J. & Kim, S.-H. (1991). *J. Appl. Cryst.* **24**, 409–411.
Kreis, W. & Hession, C. (1973). *Cancer Res.* **33**, 1862–1865.
Mamaeva, D. V., Morozova, E. A., Nikulin, A. D., Revtovich, S. V., Nikonov, S. V., Garber, M. B. & Demidkina, T. V. (2005). *Acta Cryst.* F**61**, 546–549.
Manukhov, I. V., Mamaeva, D. V., Rastorguev, S. M., Faleev, N. G., Morozova, E. A., Demidkina, T. V. & Zavilgelsky, G. B. (2005). *J. Bacteriol.* **187**, 3889–3893.
Matthews, B. W. (1968). *J. Mol. Biol.* **33**, 491–497.
Motoshima, H., Inagaki, K., Kumasaka, T., Furuichi, M., Inoue, H., Tamura, T., Esaki, N., Soda, K., Tanaka, N., Yamamoto, M. & Tanaka, H. (2000). *J. Biochem.* **128**, 349–354.
Nakayama, T., Esaki, N., Sugie, K., Beresov, T. T., Tanaka, H. & Soda, K. (1984). *Anal. Biochem.* **138**, 421–424.
Navaza, J. (1994). *Acta Cryst.* A**50**, 157–163.
Nikulin, A., Revtovich, S., Morozova, E., Nevskaya, N., Nikonov, S., Garber, M. & Demidkina, T. (2008). *Acta Cryst.* D**64**, 211–218.
Nozaki, T., Ali, V. & Tokoro, M. (2005). *Adv. Parasitol.* **60**, 1–99.
Otwinowski, Z. & Minor, W. (1997). *Methods Enzymol.* **276**, 307–326.
Rebeille, F., Jabrin, S., Bligny, R., Loizeau, K., Gambonnet, B., Van Wilder, V., Douce, R. & Ravanel, S. (2006). *Proc. Natl Acad. Sci. USA*, **103**, 15687–15692.
Sambrook, J, Fritsch, E. F. & Maniatas, T. (1989). *Molecular Cloning: A Laboratory Manual*, p. A.3. New York: Cold Spring Harbor Laboratory Press.
Sato, D., Yamagata, W., Harada, S. & Nozaki, T. (2008). *FEBS J.* **275**, 548–560.
Sato, D., Yamagata, W., Kamei, K., Nozaki, T. & Harada, S. (2006). *Acta Cryst.* F**62**, 1034–1036.
Sridhar, V., Xu, M., Han, Q., Sun, X., Tan, Y., Hoffman, R. M. & Prasad, G. S. (2000). *Acta Cryst.* D**56**, 1665–1667.
Stanley, S. Jr (2003). *Lancet*, **361**, 1025–1034.
Tanaka, H., Esaki, N. & Soda, K. (1985). *Enzyme Microb. Technol.* **7**, 530–537.
Tokoro, M, Asai, T., Kobayashi, S., Takeuchi, T. & Nozaki, T. (2003). *J. Biol. Chem.* **43**, 42717–42727.
World Health Organization (1998). *The World Health Report 1998*. Geneva: World Health Organization.
Yoshimura, M., Nakano, Y. & Koga, T. (2002). *Biochem. Biophys. Res. Commun.* **292**, 964–968.
Yoshimura, M., Nakano, Y., Yamashita, Y., Oho, T., Saito, T. & Koga, T. (2000). *Infect. Immun.* **68**, 6912–6916.

the FEBS Journal

Kinetic characterization of methionine γ-lyases from the enteric protozoan parasite *Entamoeba histolytica* against physiological substrates and trifluoromethionine, a promising lead compound against amoebiasis

Dan Sato[1,*], Wataru Yamagata[2], Shigeharu Harada[2] and Tomoyoshi Nozaki[1]

1 Department of Parasitology, Gunma University Graduate School of Medicine, Japan
2 Department of Applied Biology, Graduate School of Science and Technology, Kyoto Institute of Technology, Japan

Keywords
amoebiasis; methionine γ-lyase; site-directed mutagenesis; sulfur-containing amino acid; trifluoromethionine

Correspondence
T. Nozaki, Department of Parasitology, Gunma University Graduate School of Medicine, 3-39-22 Showa-machi, Maebashi, Gunma 371-8511, Japan
Fax: +81 27 220 8020
Tel: +81 27 220 8025
E-mail: nozaki@med.gunma-u.ac.jp
Website: http://parasite.dept.med.gunma-u.ac.jp/Enozaki_lab.html

***Present address**
Institute for Advanced Biosciences, Keio University, Tsuruoka, Yamagata, Japan

Database
Nucleotide sequence data are available in the DDBJ/EMBL/GenBank databases under the accession numbers AB094499 (EhMGL1) and AB094500 (EhMGL2)

(Received 29 August 2007, revised 13 November 2007, accepted 4 December 2007)

doi:10.1111/j.1742-4658.2007.06221.x

Methionine γ-lyase (MGL) (EC 4.4.1.11), which is present in certain lineages of bacteria, plants, and protozoa but missing in mammals, catalyzes the single-step degradation of sulfur-containing amino acids (SAAs) to α-keto acids, ammonia, and thiol compounds. In contrast to other organisms possessing MGL, anaerobic parasitic protists, namely *Entamoeba histolytica* and *Trichomonas vaginalis*, harbor a pair of MGL isozymes. The enteric protozoon *En. histolytica* shows various unique aspects in its metabolism, particularly degradation of SAAs. Trifluoromethionine (TFM), a halogenated analog of Met, has been exploited as a therapeutic agent against cancer as well as against infections by protozoan organisms and periodontal bacteria. However, its mechanism of action remains poorly understood. In addition, the physiological significance of the presence of two MGL isozymes in these protists remains unclear. In this study, we compared kinetic parameters of the wild-type and mutants, engineered by site-directed mutagenesis, of the two MGL isotypes from *En. histolytica* (EhMGL1 and EhMGL2) for various potential substrates and TFM. Intracellular concentrations of L-Met and L-Cys suggested that these SAAs are predominantly metabolized by EhMGL1, not by EhMGL2. It is unlikely that *O*-acetyl-L-serine is decomposed by EhMGLs, given the kinetic parameters of cysteine synthase reported previously. Comparison of the wild-type and mutants revealed that the contributions of several amino acids implicated in catalysis differ between the two isozymes, and that the degradation of TFM is less sensitive to alterations of these residues than is the degradation of physiological substrates. These results support the use of TFM to target MGL.

Trans-sulfuration pathways are ubiquitous and play various roles, including in the formation of Met and Cys, transmethylation reactions, and the synthesis of polyamines, antioxidants, and cofactors [1]. As there are remarkable differences in trans-sulfuration pathways between organisms, these pathways, and in

Abbreviations
CS, cysteine synthase; EhMGL, *Entamoeba histolytica* methionine γ-lyase; Hcy, homocysteine; MGL, methionine γ-lyase; OAS, *O*-acetyl-L-serine; PG, L-propargylglycine; PLP, pyridoxal 5′-phosphate; SAA, sulfur-containing amino acid; TFM, trifluoromethionine (*S*-trifluoromethyl-L-homocysteine).

particular enzymes involved in the degradation of sulfur-containing amino acids (SAAs), have been exploited as a target for chemotherapeutic intervention in cases of cancer and infectious diseases [2,3]. Methionine γ-lyase (MGL) is one such enzyme, a member of the α-family of pyridoxal 5′-phosphate (PLP)-dependent enzymes [4]. MGL catalyzes the α,γ-elimination and γ-replacement of L-Met and homocysteine (Hcy), and α,β-elimination and β-replacement of L-Cys and S-substituted analogs, and produces ammonia, α-keto acids, and volatile thiols such as hydrogen sulfide and methanethiol [5]. MGL has been characterized in several bacteria, such as *Pseudomonas putida* [6], *Clostridium sporogenes* [7], *Aeromonas* sp. [6], *Citrobacter intermedius* [8], *Citrobacter freundii* [9], *Brevibacterium linens* [10], and *Porphyromonas gingivalis* [11], parasitic protozoa such as *Trichomonas vaginalis* [12] and *Entamoeba histolytica* [13], and the plant *Arabidopsis thaliana* [14].

MGL has been implicated in the degradation of toxic SAAs [15], and also in energy metabolism through the synthesis of pyruvate or 2-oxobutyrate in *En. histolytica* [16]. Volatile thiol compounds have also been implicated in the pathogenicity *in vivo* of the periodontal bacterium, *Po. gingivalis* [11]. It has been recently shown that in *Ar. thaliana*, α-ketobutyrate and methanethiol, generated by MGL, are utilized for isoleucine biosynthesis and the production of *S*-methylcysteine, the putative storage molecule for sulfide or methyl groups, which is formed by the transfer of the acetyl moiety of *O*-acetyl-L-serine (OAS) to methanethiol [14]. Unlike bacteria and plants, *T. vaginalis* and *En. histolytica* have two isozymes of MGLs that differ distinctly in substrate specificity [13,17]. However, the physiological roles of individual isotypes as well as the significance of their redundancy remain to be elucidated.

Entamoeba histolytica, a causative agent of amoebiasis, affects an estimated 50 million people and results in 70 000 deaths per year worldwide [18]. The major clinical manifestations of amoebiasis are amoebic dysentery and extraintestinal abscesses, namely, hepatic, pulmonary and cerebral abscesses [19]. Although clinical resistance against metronidazole, the drug currently used most widely for invasive amoebiasis [3], has not yet been proven for clinical isolates, cases of treatment failure have been reported [3]. In addition, it was shown that metronidazole resistance was easily gained *in vitro* [20,21]. Moreover, metronidazole resistance is common in bacteria and the protozoan flagellates *Giardia intestinalis* and *T. vaginalis* [22]. Therefore, a novel amoebicidal drug is urgently needed.

Trifluoromethionine [*S*-trifluoromethyl-L-homocysteine (TFM)], a halogenated Met analog in which a methyl moiety is replaced by a trifluoromethyl group [23], has been shown to be highly toxic to various bacteria [24], including *Po. gingivalis* [25], *T. vaginalis* [26], and *En. histolytica* [13] (Kobayashi and Nozaki, unpublished data). TFM affected the growth of *En. histolytica* and *T. vaginalis* trophozoites at micromolar levels *in vitro* [13,26], and also cured infections in mouse and hamster models [26] (Kobayashi and Nozaki, unpublished results). The limited presence of MGL among organisms, and the remarkable differences in the toxicity of TFM against amoeba and mammalian cells [IC_{50} for *En. histolytica* trophozoites or Chinese hamster ovary cells, 18 μM [13] or 865 μM (unpublished results)], give further support for TFM as a promising lead compound for the development of new chemotherapeutics against amoebiasis.

For the further development of antiamoebic agents based on TFM, elucidation of the underlying reaction mechanisms of MGLs and the interaction of TFM with the enzymes is required. In this study, we demonstrate differences in substrate specificity and kinetic parameters for four potential natural substrates and TFM of both the wild-type and mutants, created by site-directed mutagenesis of critical amino acid residues presumed to play an important role in catalysis, of the two isotypes of *En. histolytica* MGLs (EhMGL1 and EhMGL2). The results clearly demonstrate that EhMGL1, not EhMGL2, plays the predominant role in the degradation of Met and Cys in the amoeba trophozoites, whereas OAS seems to be decomposed by neither EhMGL1 nor EhMGL2. Our results also show that TFM is mainly degraded by EhMGL2, but not by EhMGL1. In addition, the contributions of the amino acids implicated in previous studies [17,27,28] to the catalysis of individual physiological and deleterious substrates differ greatly between the two EhMGL isotypes. The information provided by the present study should help in the further rational design of novel chemotherapeutic agents targeting MGL against amoebiasis.

Results and Discussion

Expression and purification of the genetically engineered wild-type of EhMGL1

We were unable to precisely determine kinetic constants for the reaction catalyzed by MGL isotypes from *En. histolytica*, due to the heterogeneity of EhMGL1 in the previous preparation [13] (approximately 20% of EhMGL1 was produced as a 35 kDa truncated form; Fig. 1A, lane 1). Our attempt to

Fig. 1. (A) Purified proteins (1.0 μg) were analyzed by 12% SDS/PAGE under reducing conditions, and stained with Coomassie brilliant blue. Lane 1: wild-type MGL1. Lane 2: nucleotide-substituted MGL1. Lane 3: MGL2. Molecular mass markers are indicated on the right. (B) Partial alignment of EhMGL1. Wild-type MGL1 (upper), nucleotide-substituted MGL1 (middle) and the deduced amino acids (lower) are aligned. The five substituted nucleotides are indicated in lower-case on a black background. A box represents the N-terminal end of the truncated sequence determined by Edmann degradation. The incidental Shine–Dalgarno-like sequence is underlined.

further purify the full-length EhMGL1 with anion exchange and gel filtration chromatography failed (data not shown), suggesting that the truncated EhMGL1 probably forms a heterogeneous tetrameric complex with the full-length EhMGL1. We determined the N-terminus of the truncated EhMGL1 to be Gly46 (Fig. 1B, boxed) by Edmann degradation of the 35 kDa band excised from the SDS/PAGE gel, and postulated that the truncation was caused by a fortuitous initiation of translation at Met45 due to the similarity of the nucleotide sequence upstream of Met45 of EhMGL1 to the Shine–Dalgarno sequence (Fig 1B, underlined). The truncated enzyme lacking a glutathione *S*-transferase tag was purified by affinity chromatography, indicating that the full-length version and the truncated version form a tetramer. The truncation is potentially deleterious to the stability and activity of a tetramer, because this region is involved in a dimer–dimer interaction and catalytic reaction (e.g. *Ps. putida* MGL [28]). To eliminate the production of the truncated EhMGL1, we replaced five nucleotides within this region of the *EhMGL1* gene without causing amino acid substitutions (Fig. 1B, white lower-case on a black background), and applied the engineered EhMGL1 to protein expression. This genetically engineered EhMGL1 was purified to > 95% homogeneity without traceable contamination of the truncated form (Fig. 1A, lane 2).

Comparison of the specific activity and kinetic parameters for potential substrates between the wild-type MGL isotypes

To understand the specific roles of the two MGL isotypes, which show 69% mutual identity [13], and also to demonstrate differences between them in reaction mechanisms towards physiological substrates and TFM, we determined the apparent specific activity (with a constant substrate concentration of 2 mM) and the kinetic parameters of recombinant EhMGL1 and EhMGL2 (Tables 1 and 2). Despite the heterogeneity of the EhMGL1 preparation used in the previous study [13], the kinetic constants of EhMGL1 in the present study largely agreed with the previous data, except that the relative activity towards Cys and OAS was underestimated by 4–5-fold previously (the relative specific activities of EhMGL1 towards Cys and OAS were 19.7% and 11.1% relative to that towards Met [13], and 116% or 42.4% in the present study). The discrepancy in the kinetic constants of EhMGL1 was probably attributable to the heterogeneity of the EhMGL1 preparation in the previous study. The V_{max}

Table 1. Specific activities of wild-type and mutant EhMGL1 (A) and EhMGL2 (B). Apparent specific activity (mean ± SD in triplicate) is shown as μmol of α-keto acid produced·min^{-1}·mg^{-1} protein. ND, activity not detected (less than 0.05 μmol of product per min per mg of protein).

(A)

Substrate	Wild-type	Y108F	C110S	C110G	R55A
L-Methionine	1.39 ± 0.01	0.23 ± 0.02	1.11 ± 0.08	0.56 ± 0.04	ND
Trifluoromethionine	1.16 ± 0.10	2.54 ± 0.28	4.78 ± 0.19	1.61 ± 0.10	1.01 ± 0.15
DL-Homocysteine	1.83 ± 0.26	0.38 ± 0.05	1.18 ± 0.05	0.77 ± 0.02	ND
L-Cysteine	1.61 ± 0.35	0.52 ± 0.06	1.06 ± 0.26	1.12 ± 0.12	0.10 ± 0.01
O-Acetyl-L-serine	0.59 ± 0.12	0.67 ± 0.09	0.29 ± 0.04	0.82 ± 0.01	0.14 ± 0.02

(B)

Substrate	Wild-type	Y111F	C113S	C113G	R58A
L-Methionine	0.71 ± 0.02	ND	0.06 ± 0.0001	0.08 ± 0.002	ND
Trifluoromethionine	14.03 ± 2.03	7.76 ± 1.05	8.14 ± 0.70	14.67 ± 0.54	0.78 ± 0.05
DL-Homocysteine	7.42 ± 1.02	0.64 ± 0.17	1.90 ± 0.11	2.34 ± 0.06	ND
L-Cysteine	0.62 ± 0.02	0.15 ± 0.01	0.09 ± 0.01	0.75 ± 0.03	ND
O-Acetyl-L-serine	0.37 ± 0.04	0.26 ± 0.02	0.06 ± 0.01	0.90 ± 0.05	ND

(or the specific activity) of EhMGL2 against DL-Hcy previously reported (V_{max}, 1.31 μmol product·min^{-1}·mg^{-1} protein; relative specific activity compared to that against Met, 162%) was also underestimated (k_{cat}, 10.56 s^{-1}; relative specific activity 10.5-fold higher than that for Met, in the present study). In addition, the K_m of EhMGL2 for OAS in the previous study (0.89 mM) disagreed with that in the present study (52.33 mM). We assumed that these differences were attributable to the assay methods used; the α-keto acid assay was employed in the present study, whereas the nitrogen assay, which has less sensitivity, was used previously. Taken together, the specificities of the two isotypes are briefly summarized as follows. EhMGL1 showed comparable (within 1.1–3.1-fold differences) specific activities towards OAS and all SAAs tested in this study (0.59–1.83 μmol product·min^{-1}·mg^{-1} protein), whereas EhMGL2 showed 10–20-fold more activity with DL-Hcy than with other substrates (7.42 and 0.37–0.71 μmol product·min^{-1}·mg^{-1} protein, respectively).

The K_m of EhMGL2 for Met (3.58 mM) is six-fold higher than that of EhMGL1 (0.61 mM). In addition, the k_{cat} for Met of EhMGL1 is 1.6-fold higher than that of EhMGL2. The k_{cat}/K_m, which indicates the catalytic efficiency [29], of EhMGL1 is 10-fold higher than that of EhMGL2. Taking into account the intracellular Met concentrations, measured by NMR (2.1 ± 0.6 mM) or direct amino acid analysis (0.8 mM, [30]), we speculate that EhMGL1, but not EhMGL2, is involved in the degradation of Met under normal conditions. Similarly, the 2.0-fold higher k_{cat} and 2.7-fold lower K_m for Cys of EhMGL1 than of EhMGL2, together with the intracellular Cys concentration (0.4 mM [30]), suggest that EhMGL1, but not EhMGL2, mainly catalyzes the degradation of Cys *in vivo*. Although Hcy is an essential component of the Met cycle [15], it is believed that Hcy must be maintained at low concentrations to avoid toxicity [31]. The intracellular Hcy concentration is unknown in amoebae, but is presumed to be several micromoles per liter, as shown for human plasma [32], a much lower concentration than the K_m of EhMGL1 and EhMGL2 for Hcy (1.5–3.0 mM). Thus, although the k_{cat}/K_m for Hcy of EhMGL2 was 5.5-fold higher than that of EhMGL1, the assumed Hcy concentrations suggest that neither EhMGL plays a significant role in the elimination of Hcy under physiological conditions.

Kinetic parameters against OAS also revealed that the two EhMGLs have discernible catalytic properties (EhMGL1, 6.28 mM and 1.74 s^{-1}, and EhMGL2, 52.33 mM and 6.22 s^{-1}, for K_m and k_{cat}, respectively). Although the intracellular OAS concentration is unknown for amoebae, the presence of multiple isotypes of cysteine synthase (CS) makes it unlikely that EhMGLs are involved in the degradation of OAS. CS, which generates Cys from H_2S and OAS, has advantages (e.g. K_m and k_{cat} of EhCS1 are 1.27 mM and 395 s^{-1}, respectively) for OAS, as compared to EhMGLs [33]. Three isotypes of CS are constitutively expressed, as shown by immunoblotting [34] and a transcriptome analysis with a DNA microarray [35]. Thus, OAS is most likely utilized predominantly by CS. Taken together, these findings suggest that EhMGL1 is responsible for the decomposition and the maintenance of the cellular concentrations of Met and Cys, whereas the physiological substrates of EhMGL2 under normal growth conditions remain unknown.

Table 2. Kinetic parameters of wild-type and mutant EhMGL1 (A) and EhMGL2 (B). Kinetic parameters were measured with at least five different concentrations. Values are means ± SD in triplicate. ND, not detectable; NT, not tested.

(A)

	Wild-type			Y108F			C110S			C110G			R55A		
Substrate	K_m (mM) ± SD	k_{cat} (s^{-1}) ± SD	k_{cat}/K_m	K_m (mM) ± SD	k_{cat} (s^{-1}) ± SD	k_{cat}/K_m	K_m (mM) ± SD	k_{cat} (s^{-1}) ± SD	k_{cat}/K_m	K_m (mM) ± SD	k_{cat} (s^{-1}) ± SD	k_{cat}/K_m	K_m (mM) ± SD	k_{cat} (s^{-1}) ± SD	k_{cat}/K_m
L-Methionine	0.61 ± 0.06	1.82 ± 0.11	2.99	NT	NT	NT	0.72 ± 0.02	0.93 ± 0.15	1.29	0.19 ± 0.01	0.36 ± 0.03	1.91	NT	NT	NT
Trifluoromethionine	0.10 ± 0.00	0.81 ± 0.08	8.02	0.57 ± 0.02	2.22 ± 0.08	3.88	NT	NT	NT	NT	NT	NT	0.83 ± 0.05	1.26 ± 0.06	1.52
DL-Homocysteine	3.03 ± 0.06	3.92 ± 0.15	1.30	NT	NT	NT	NT	NT	NT	NT	NT	NT	NT	NT	NT
L-Cysteine	0.64 ± 0.01	1.59 ± 0.14	2.48	1.01 ± 0.07	0.67 ± 0.06	0.66	0.46 ± 0.05	0.78 ± 0.03	1.69	0.34 ± 0.02	1.01 ± 0.02	3.00	NT	NT	NT
O-Acetyl-L-serine	6.28 ± 0.53	1.74 ± 0.12	0.28	NT	NT	NT	NT	NT	NT	NT	NT	NT	NT	NT	NT

(B)

	Wild-type			Y111F			C113S			C113G			R58A		
	K_m (mM) ± SD	k_{cat} (s^{-1}) ± SD	k_{cat}/K_m	K_m (mM) ± SD	k_{cat} (s^{-1}) ± SD	k_{cat}/K_m	K_m (mM) ± SD	k_{cat} (s^{-1}) ± SD	k_{cat}/K_m	K_m (mM) ± SD	k_{cat} (s^{-1}) ± SD	k_{cat}/K_m	K_m (mM) ± SD	k_{cat} (s^{-1}) ± SD	k_{cat}/K_m
L-Methionine	3.58 ± 0.30	1.11 ± 0.13	0.31	NT	NT	NT	15.12 ± 0.24	0.47 ± 0.05	0.03	ND[a]	ND[a]	ND[a]	NT	NT	NT
Trifluoromethionine	0.92 ± 0.06	17.46 ± 1.21	19.05	0.29 ± 0.0003	5.80 ± 0.54	20.29	NT	NT	NT	NT	NT	NT	1.62 ± 0.15	1.19 ± 0.11	0.73
DL-Homocysteine	1.47 ± 0.12	10.56 ± 1.25	7.19	NT	NT	NT	NT	NT	NT	NT	NT	NT	NT	NT	NT
L-Cysteine	1.70 ± 0.09	0.80 ± 0.08	0.47	ND	NT	NT	5.45 ± 0.09	0.24 ± 0.01	0.04	ND[a]	ND[a]	ND[a]	NT	NT	NT
O-Acetyl-L-serine	52.33 ± 1.52	6.22 ± 0.61	0.12	NT	NT	NT	NT	NT	NT	NT	NT	NT	NT	NT	NT

[a] K_m is estimated to be less than 0.1 mM.

Kinetic parameters of mutants of the two MGL isotypes

Among the several amino acid residues shown to interact with PLP, the importance of a few was evaluated in the amoebic MGL isotypes. Our preliminary crystallographic study suggests that Tyr111, Cys113 and Arg58 of EhMGL2 are oriented towards PLP in close proximity [36] (data not shown). Tyr114 of *Ps. putida* MGL (corresponding to Tyr108 and Tyr111 of EhMGL1 and EhMGL2, respectively) was implicated in γ-elimination, attacking the γ-position of a substrate as an acid catalyst [14]. Cys110 and Arg55 of EhMGL1, which correspond to Cys113 and Arg58 of EhMGL2, are also predicted to be located in similar positions.

MGL1(Y108F) and MGL2(Y111F) showed a 79–100% reduction in the α,γ-elimination of both Met and Hcy as compared to the wild-type MGLs, whereas these mutations only slightly affected the α,β-elimination of OAS (a 1.14-fold increase or only a 28% reduction as compared to wild-type MGL1 or MGL2, respectively). These results were similar to the Tyr114 mutant of *Ps. putida* MGL [27]. Unlike the case of OAS, MGL1(Y108F) and MGL2(Y111F) showed reduced α,β-elimination for Cys (68% or 76% reduction); for example, MGL1(Y108F) showed a 1.6-fold increase in the K_m and a 58% decrease in the k_{cat} for Cys. This implies that the hydroxyl group of Tyr108 of EhMGL1 is actively involved in the β-elimination and γ-elimination of the C–S bond, but not the β-elimination of the C–O bond, of OAS.

The Cys near the active site was shown to be important for activity by chemical modification with 2-nitrothiocyanobenzoic acid and labeling with a PLP analog, *N*-(bromoacetyl)pyridoxamine phosphate, in *Ps. putida* MGL [37,38]. Cys116 was shown to be located in close proximity to Tyr114 [28]. This Cys is not conserved in other PLP α-family enzymes; Cys is substituted by Gly or Pro in cystathionine γ-lyase, cystathionine β-lyase, and cystathionine γ-synthase [27,28]. In *B. linens* MGL, Gly is substituted for Cys at this position. *B. linens* MGL degrades neither Cys nor cystathionine [10], whereas *Ar. thaliana* MGL decomposes Cys but degrades cystathionine only marginally, in spite of the presence of Gly at this position [39]. The Cys to Ser or Thr mutations of *Ps. putida* MGL caused a reduction in activity [28]. Neither *En. histolytica* MGL nor *T. vaginalis* wild-type MGL degrades cystathionine [13,17]. The Cys → Gly mutation of *T. vaginalis* MGLs reduced γ-elimination activity towards Met and Hcy 5–13-fold, but only slightly changed β-elimination activity for Cys and OAS (0.38–2.5-fold) [17]. Thus, it was proposed that this Cys plays an important role in substrate specificity, i.e. the preference of substrates for γ-elimination in *T. vaginalis* MGLs.

Amoebic MGL2(C113S) showed reduced activities towards Met, Cys, and Hcy (9–26% of that of the wild-type), whereas MGL1(C110S) showed only a marginal reduction (65–80% of that of the wild-type). MGL1(C110S) and MGL2(C113S) showed reduced k_{cat} values for Met or Cys (49–51% or 29–42% of that of wild-type MGL1 or MGL2, respectively), whereas the K_m values remained unchanged for MGL1(C110S) (72–118% of that of the wild-type) or increased 3.2–4.2-fold for MGL2(C113S). In contrast to the Cys → Ser mutation, the Cys → Gly mutation caused 2.5-fold and 1.4-fold increases in activity towards OAS for MGL1(C110G) and MGL2(C113G), respectively. MGL2(C113G) also showed a 20% higher level of activity towards Cys than wild-type MGL2. Interestingly, the K_m values of MGL1(C110G) for Met and Cys were reduced by 70% and 48%, respectively. In contrast, the k_{cat} values of MGL1(C110G) for Met and Cys decreased by 80% and 34%, respectively. Additionally, MGL1(C110G)-catalyzed reactions of Met or Cys showed saturation with 0.125 M substrate, suggesting the K_m to be < 0.1 mM (Table 1, indicated by asterisks). Taken together, these findings show that the contribution of this Cys to the catalytic reaction clearly differs between EhMGL1 and EhMGL2; Cys113 of MGL2 is heavily involved in substrate specificity, whereas Cys110 of MGL1 is not so essential for catalysis. However, as mutations of Cys110 of MGL1 produced 56% and 32% reductions in the specificity constants with Met and Cys, respectively, this residue might be also important for catalysis.

Arg55 of EhMGL1 and Arg58 of EhMGL2 are located near the PLP of the neighboring subunit of the catalytic dimer, as revealed by X-ray crystallography (unpublished data), similar to what is found for MGLs from *Ps. putida* [28] and *Ci. freundii* [40]. The mutation of this Arg to Ala was shown to abolish the activity for Met of *Ps. putida* MGL [28]. Similarly, the R58A mutation of MGL2 completely abolished activity towards Met, Cys, Hcy, and OAS, whereas residual activity remained for MGL1(R55A) towards Cys and OAS, but not Met and Hcy. We confirmed by gel filtration that the apparent molecular mass of MGL1(R55A) and MGL2(R58A) was approximately 175 kDa, similar to that of wild-type MGLs (data not shown). Thus, interference with dimerization was not a reason for the observed loss of activity. It was also shown that a mutant containing the corresponding Arg mutation formed a tetramer in *Ps. putida* MGL

[28]. It is worth considering the utilization of MGL1(R55A) and MGL2(R58A) mutants for dominant negative effects, because these EhMGL mutants were shown to be associated with endogenous EhMGL in a heterotetrameric complex (data not shown).

Kinetic parameters of MGL wild-type and mutants towards TFM

The specific activity of EhMGL2 against TFM was 12-fold higher than that of EhMGL1. This increase is mostly attributable to a large difference in k_{cat}; the k_{cat} of EhMGL2 was 21-fold higher than that of EhMGL1 (17.5 s^{-1} and 0.81 s^{-1}). By contrast, the K_m of EhMGL2 was nine-fold higher than that of EhMGL1 (0.92 and 0.10 mM, respectively). Thus, the catalytic efficiency, expressed as k_{cat}/K_m, of EhMGL2 is only 2.4-fold higher than that of EhMGL1 (19.05 and 8.02, respectively; Table 2). It is remarkable that the k_{cat} of EhMGL1 for TFM was comparable to that for Met and Cys, whereas the k_{cat} of EhMGL2 for TFM was 16–22-fold higher than that for these physiological substrates. The K_m of EhMGLs for TFM was 52–470-fold lower than that of the closest mammalian counterpart (rat liver cystathionine γ-lyase, K_m = 48 mM) [41].

None of the mutations examined in this study, except for MGL2(R58A), greatly affected the activity towards TFM, suggesting that the mechanism of the MGL-catalyzed reaction of TFM is relatively independent of these amino acids, unlike the case for physiological substrates. The activity of MGL2(R58A) towards TFM was similar to that of wild-type MGL for the physiological substrates. Moreover, the effects of the Y108F substitution on the K_m and k_{cat} of EhMGL1 for TFM are opposite to those of Y111F of EhMGL2; the K_m and k_{cat} of EhMGL1(Y108F) increased 5.6-fold and 2.7-fold, respectively, as compared to those of wild-type EhMGL1, whereas the K_m and k_{cat} of EhMGL2(Y111F) decreased threefold. The Tyr → Phe mutation caused only a 2.1-fold reduction in the catalytic efficiency (k_{cat}/K_m) of EhMGL1 (8.02 to 3.88), whereas the corresponding mutation of EhMGL2 did not have a significant effect (19.05 to 20.29). The degradation of TFM probably proceeds without interaction with Tyr111, Cys113, and Arg58 (in the case of EhMGL2), possibly due to the electronegativity of the trifluoromethyl group of TFM. It is also worth noting that the role of Tyr108 (or Tyr111) in the degradation of TFM significantly differs between EhMGL1 and EhMGL2.

As indicated, EhMGL2, but not EhMGL1, displayed a remarkable preference for TFM. Although elucidation of the mechanisms responsible for this observation await further study, we speculate that the preference is associated with the functional group bound to the γ-carbon: the trifluoromethyl moiety. EhMGL2 also showed a remarkable preference for Hcy, similar to TFM. Three fluorides on the methyl carbon of TFM and a sulfur atom of the thiol group of Hcy may participate in the formation of additional hydrogen bonds in the catalytic pocket. Although we previously reported X-ray crystallography of EhMGL2 [36], EhMGL2 cocrystallized with either TFM or Hcy has not yet been obtained.

Crosslinking of EhMGLs and a scavenger protein by TFM

It was previously proposed that a thiol derived from the degradation of TFM by MGL, carbonothionic difluoride, crosslinks the primary amino group of proteins, which results in toxicity [41]. This model was supported by the detection of released fluoride, a byproduct of crosslinking with carbonothionic difluoride [41]. We attempted to directly demonstrate that TFM-derived product(s) causes protein modification. We investigated whether the recombinant EhMGL was modified after the incubation with TFM by examining the mobility of the proteins by SDS/PAGE. When recombinant EhMGL1 or EhMGL2 was incubated with TFM, at least three additional bands were found (Fig. 2A, lane 1, open arrowheads). Incubation of EhMGLs with Met or without substrates did not result in the appearance of these bands (Fig. 2A, lanes 2 and 3). Preincubation of EhMGLs with L-propargylglycine (PG), a suicide substrate of PLP–enzyme, prior to the mixing with TFM, abolished these extra bands (Fig. 2A, lane 4). Immunoblot assay with antibody to EhMGL2 (Fig. 2C) showed that when EhMGL1 was reacted with TFM, but not with Met, or pretreated with PG, EhMGL1 was no longer recognized by the antibody (the equal loading of proteins was verified by silver staining; Fig. 2A), suggesting that EhMGL1 was chemically altered by unknown modifications caused by the decomposition of TFM catalyzed by MGL. Suppression of the antibody's reactivity by the treatment with TFM was also observed for EhMGL2, but not for EhMGL1. The additional bands described above (open arrowheads) were not recognized by the antibody, suggesting that these bands were also chemically modified. Alternatively, these bands were not derived from EhMGLs, but were minor contaminants in the recombinant protein preparations. To examine whether irrelevant proteins can also serve as scavengers of carbonothionic difluoride produced from TFM by

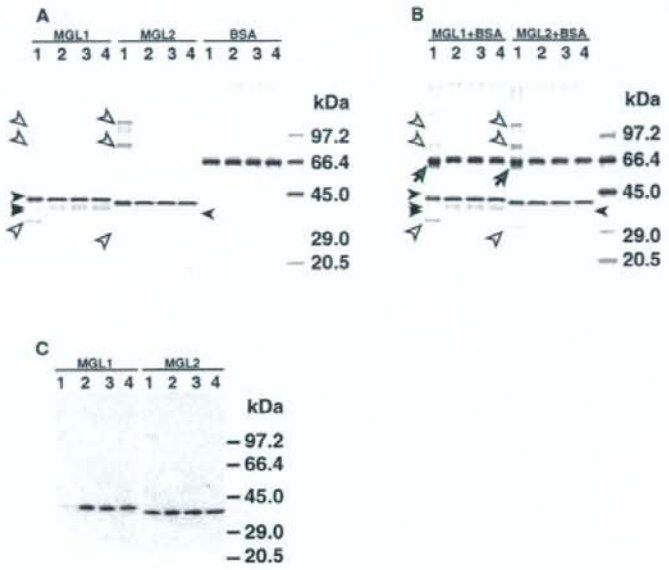

Fig. 2. *In vitro* crosslinking by TFM produced by recombinant MGLs. (A) The recombinant EhMGL1 or EhMGL2 or BSA was preincubated with 4 mM PG (lane 4) or without PG (lanes 1–3) for 30 min at 37 °C, and incubated with 4 mM TFM (lanes 1 and 4), Met (lane 2) or 2.5% dimethylsulfoxide (control, lane 3) in 100 mM sodium phosphate (pH 7.0) containing 20 μM PLP and 1 mM dithiothreitol for 1 h at 37 °C. The reaction mixtures containing 50 ng of EhMGL or 100 ng of BSA were electrophoresed on a 5–20% SDS/PAGE gel under reducing conditions, and subjected to silver staining. (B) The same reactions were performed with the mixtures of EhMGL and BSA. (C) The reaction mixtures of (A) were subjected to immunoblot analysis with antibody to EhMGL1 (left) or EhMGL2 (right). One-fourth of the volume of each reaction mixture (corresponding to 25 ng of EhMGL) was analyzed. Open arrowheads, filled arrowheads and gray arrows depict the bands that appeared upon incubation with TFM, contaminants of MGL preparations, and a smeared band probably corresponding to crosslinked BSA, respectively. Molecular mass markers are indicated on the right.

EhMGLs, MGL was incubated with TFM in the presence or absence of BSA, electrophoresed, and silver-stained or immunoblotted with antibody to EhMGL2 (Fig. 2B). Although we did not observe BSA-derived extra bands, the band corresponding to BSA on a silver-stained gel was smeared only when BSA was incubated with TFM and EhMGLs (gray arrows), suggesting that unknown modifications or degradation of BSA probably occurred.

As we observed differences in reactivity with the TFM-derived product between the two EhMGLs, we examined whether the sensitivities of the two EhMGLs to inactivation by TFM differ. We preincubated EhMGLs with TFM at a molecular ratio of 1 : 1000, and further tested for the Met-degrading activity on the basis of the detection of α-keto acid after the addition of 2 mM Met (Fig. 3). Approximately 85% of EhMGL2 activity remained after 1 h, whereas 75% of EhMGL1 activity was lost. MGL activity following preincubation with Met was indistinguishable from that without preincubation, confirming that the decrease was not due to inactivation of MGL during the preincubation. These results clearly showed that significant differences in sensitivity to TFM exist between the two EhMGLs. Although we did not identify specific proteins that were crosslinked and inactivated *in vivo* by the MGL-mediated degradation of TFM, except for the amoebic MGL itself, we speculate that carbonothionic difluoride generates crosslinks surrounding proteins in the cytosol of the parasite, leading to the observed toxicity to the cell.

The fact that EhMGL2, which is more active in the degradation of TFM, is less sensitive than EhMGL1 seems to contradict the notion that the product of the degradation is the enzyme inactivator. However, we speculate that the distribution of possible primary amines, which are target of the TFM adducts (carbonothionic difluoride), in close proximity to the catalytic pocket differs between MGL1 and MGL2, and that this difference may influence the sensitivity to the

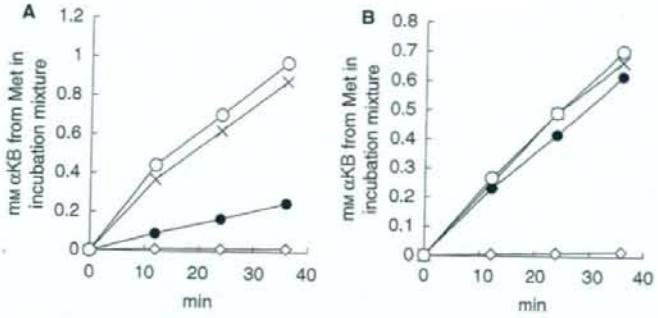

Fig. 3. Inactivation of MGL by incubation with TFM. The recombinant EhMGL1 [(A) 15 ng·μL^{-1}] or EhMGL2 [(B) 30 ng·μL^{-1}] was preincubated with 0.35 mM or 0.7 mM TFM respectively (filled circles), PG (diamonds), Met (crosses) or control (0.625% dimethylsulfoxide) (open circles) at 37 °C for 1 h. After preincubation, the mixtures were further incubated with 2 mM Met for 0, 12, 24 or 36 min, and the amount of α-keto acid was measured. The means for the triplicate measurements of the amount of α-keto acids produced after the addition of 2 mM Met are plotted. Error bars are omitted for clarity (standard errors < 0.03).

inactivation by the TFM adducts. A comparison of primary structures indicated that 28 basic amino acids (i.e. Lys and Arg) were conserved, whereas eight and 12 are unique to MGL1 and MGL2, respectively [13]. Thus, these eight MGL1-specific Lys and Arg residues may be involved in the inactivation by TFM adducts.

Roles of two MGL isotypes in *En. histolytica*

The kinetic parameters of the two MGL isotypes suggest that EhMGL1 is the primary isotype involved in the degradation of Met and Cys. Both an immunoblot study [13] and a transcriptome analysis (supplemental data of [35]) showed that EhMGL1 and EhMGL2 were expressed at comparable levels. To directly confirm the *in vivo* activity of the two isozymes in the parasite, we measured specific activities of MGL in the amoebic extracts using two representative physiological substrates, i.e. Met and Hcy. The specific activities with Met and Hcy in the parasite lysate (the 15 000 *g* supernatant fraction) were 0.456 and 2.28 nmol of product·min^{-1}·mg^{-1} of lysate, respectively. Assuming that the substrate specificity is similar between native and recombinant EhMGLs and that recombinant EhMGLs are fully active, the EhMGL1/EhMGL2 ratio was determined to be 1 : 1.38 (data not shown). This ratio agreed well with the data from the immunoblot and transcriptome analyses. The constitutive expression of EhMGL1 and EhMGL2 *in vitro* ([13] and this study) and *in vivo* [35] strongly suggests that both isotypes play indispensable and nonoverlapping roles during proliferation and intestinal infection. As the K_m of EhMGL2 for most naturally occurring SAAs and related compounds was significantly higher than that of EhMGL1, the physiological substrates of EhMGL2 and precise biological role of MGL2 *in vivo* under normal growth conditions are still not well understood. However, it is conceivable that EhMGL1 plays a central role in the control of SAA concentrations in the cell under normal conditions, whereas EhMGL2 is involved in the control of SAA homeostasis in cases where intracellular SAA concentrations are elevated to toxic levels, e.g. on exposure to high concentrations of Cys precursors, including Ser, or the engulfment of excessive amounts of bacteria or host cells. This can be interpreted as follows to explain the regulatory mechanism of the intracellular Met concentration. Under physiological Met or Cys concentrations, EhMGL1 is fully active, whereas EhMGL2 is only partially active, due to its higher K_m and lower k_{cat}/K_m. However, at higher Met concentrations, EhMGL2 plays an supplementary role in reducing the concentration of this toxic amino acid. In addition, EhMGL2 may be present specifically to degrade Hcy. Gilchrist *et al.* [35] reported that EhMGL1 was overexpressed 15-fold at the mRNA level 1 day after amoebae were inoculated into the mouse cecum, but not a month later, when they colonized the intestine (only 1.3-fold increase), whereas EhMGL2 mRNA was repressed 1.8–4.2-fold during this period [35], suggesting that the expression of EhMGL1 is induced under stress conditions. We also speculate that EhMGL2 may prefer substrates other than those used in this study, e.g. *S*-adenosylmethionine, *S*-adenosylhomocysteine, and *S*-methylmethionine. The reaction catalyzed by MGLs is considered to be unidirectional, because one of the products from Met, methanethiol, is highly volatile and immediately evaporates extracellularly [25].

However, as it is not reasonable to speculate that *En. histolytica* discharges methanethiol, while it incorporates sulfide, we propose that *En. histolytica* salvages methanethiol. This is plausible if *En. histolytica* possesses a pathway to produce Cys from Met in which MGL is used to provide reactive thiol molecules such as sulfide and methanethiol, which are in turn utilized as substrates to form Cys and *S*-methylcysteine as proposed for *Ar. thaliana* [14]. One of the major thiols produced by amoebic MGLs, hydrogen sulfide, is probably assimilated to form Cys in a reaction also catalyzed by CS [34]. This organism has three isozymes of CS [42], which convert OAS and hydrogen sulfide to Cys [15]; one of these may utilize methanethiol instead of hydrogen sulfide as an alanyl acceptor. Genes encoding enzymes that utilize methanethiol as a substrate, such as *O*-acetylhomoserine sulfhydrylase (EC 2.5.1.49) and methanethiol oxidase (EC 1.8.3.4), are not present in the *En. histolytica* database. Metabolomics or fluxomics using amoebic transformants overexpressing EhMGL1 or EhMGL2 should elucidate the physiological substrates and functions of these enzymes.

The excellent reactivity of TFM, a promising lead to target MGL

We demonstrated in this study that TFM is an ideal lead compound as a prodrug targeting MGL, from an enzymological point of view. The excellent ability of TFM to act as a prodrug is primarily attributable to the high k_{cat} and low K_m of MGL2 against TFM. It is considered that both EhMGL1 and EhMGL2 are, despite their clear differences in K_m and k_{cat}, probably responsible for the decomposition of TFM, because the concentration that is effective against the amoebae is two orders of magnitude lower than the K_m values. It was reported that the incorporation of TFM into proteins and recycling via the Met cycle are extremely poor [43,44], which reinforces the notion that TFM and its derivatives are not very toxic to mammalian cells (data not shown). Finally, the elucidation of reaction mechanisms against both physiological substrates and prodrugs such as TFM should provide a rationale for the further design of TFM derivatives.

Experimental procedures

Chemicals

All chemicals of analytical grade were purchased from Wako Pure Chemical Industries (Osaka, Japan) or Sigma-Aldrich (St Louis, MO, USA) unless otherwise stated. PG was purchased from PepTech Corp. (Burlington, MA, USA). TFM was a gift from T. Toru and N. Shibata (Graduate School of Engineering, Nagoya Institute of Technology, Nagoya, Japan).

Mutagenesis, expression and purification of recombinant enzymes

To eliminate the production of a truncated EhMGL1 in *Escherichia coli*, due to the fortuitous translation initiation at the second Met (Met45) within the coding region, five synonymous nucleotide changes were introduced into EhMGL1 (accession number AB094499). Nested PCR was performed with appropriate oligonucleotide primers (supplementary Table S1) and pGEX6P1–EhMGL1 [13] as template, and subsequently with primers having *Bam*HI and *Xba*I sites for 'nested PCR', using the first PCR product as template. To make use of the *Bam*HI site in the vector and the *Xba*I site in the EhMGL1 gene, the product of the nested PCR was replaced with the corresponding region in pGEX–EhMGL1 [13] to produce pGEX–EhMGL1fl. The following mutations were introduced into EhMGL1 and EhMGL2 (AB094500), using the GeneTailor site-directed mutagenesis system (Invitrogen, Carlsbad, CA, USA): Y108F, C110S, C110G and R55A in EhMGL1; and Y111F, C113S, C113G and R58A in MGL2. PCRs were performed with the corresponding oligonucleotide primers (supplementary Table S1) and methylated pGEX–EhMGL1fl and pGEX–EhMGL2 [13] as templates. The transformation and selection of mutated plasmids were performed according to the instructions of the manufacturer. Both wild-type and mutated proteins were expressed and purified as described previously [13,36].

Activity assay and measurement of kinetic parameters

The MGL activity was measured on the basis of the production of α-keto acids [45]. Assays were carried out in 60 μL of 100 mM sodium phosphate (pH 7.0) containing 1 mM dithiothreitol and 20 μM PLP, and 3–60 $\mu g \cdot mL^{-1}$ of the recombinant enzymes, at 37 °C for 10 min. The ranges of substrate concentrations for the measurement of kinetic parameters were 0.125–20 mM for Met, Cys, OAS, and TFM, and 0.125–2 mM for Hcy. Specific activity with 2 mM substrates was also measured. These measurements were performed independently. To assay the activity of MGLs in the parasite, amoeba cells were lysed with 100 mM sodium phosphate (pH 7.0) containing 20 μM PLP and 0.1% Triton X-100. The insoluble materials were eliminated by centrifugation at 15 000 *g* for 10 min, and subsequently 12.4 and 1.24 $mg \cdot mL^{-1}$ of the supernatant was incubated with 2 mM Met and Hcy, respectively. After the reaction

was terminated by the addition of 6 μL of 50% trichloroacetic acid, the solution was centrifuged at 15 000 *g* for 10 min at 4 °C, and 39.3 μL of the supernatant was incubated with 110 μL of 0.33 M sodium acetate (pH 5.0) containing 1.55 mM 3-methyl-2-benzothiazolinone hydrazone hydrochloride hydrate for 1 h at 50 °C. The amounts of azines generated were estimated by measuring absorbance at 320 nm [45], with pyruvic acid and sodium 2-oxobutyrate as standards. The kinetic parameters were estimated using Hanes–Woolf plots.

Crosslinking of recombinant MGLs

The purified recombinant MGL1 or MGL2 (at a final concentration of 60 ng·μL^{-1} each) was incubated with 1 mM TFM or Met in 100 mM sodium phosphate (pH 7.0) containing 20 μM PLP in the presence or absence of 120 ng·μL^{-1} BSA for 1 h at 37 °C. For some experiments, the recombinant MGLs were preincubated with 10 mM PG for 30 min at 37 °C before the substrates were added. The reaction mixtures were electrophoresed on a 5–20% gradient SDS/PAGE gel under reducing conditions, and proteins were detected with silver staining and immunoblot analysis with antibody to MGL1 or MGL2 [13].

Measurement of remaining MGL activity after the incubation with TFM

The recombinant MGL1 (15 ng·μL^{-1}) and MGL2 (30 ng·μL^{-1}) were mixed with 0.35 mM or 0.7 mM TFM, PG and Met at 37 °C in 100 mM sodium phosphate (pH 7.0) containing 20 μM PLP. The molar ratio of MGL to substrate or inhibitor was maintained at 1 : 1000. After 1 h of preincubation, 2 mM Met was added, and the amount of α-keto acid was measured after 0, 12, 24 and 36 min, as described above. After the amount of α-ketobutyric acid produced in the preincubation mixture was subtracted, the estimated amount of α-keto acid generated after the addition of 2 mM Met was plotted.

Acknowledgements

The authors thank Kayoko Hashimoto and Rumiko Kosugi for technical assistance and Norio Shibata and Takeshi Toru, Nagoya Institute of Technology, for the synthesis of TFM and constructive discussions. This work was supported in part by Grants-in-Aid for Scientific Research from the Ministry of Education, Culture, Sports, Science and Technology of Japan (17390124, 17790282, 18050006, and 18073001), a grant for Research on Emerging and Re-emerging Infectious Diseases from the Ministry of Health, Labour and Welfare (01712004), and a grant for the Project to Promote the Development of Anti-AIDS Pharmaceuticals from the Japan Health Sciences Foundation (KA11501) to T. Nozaki.

References

1 Brosnan JT & Brosnan ME (2006) The sulfur-containing amino acids: an overview. *J Nutr* **136**, 1636S–1640S.
2 Cellarier E, Durando X, Vasson MP, Farges MC, Demiden A, Maurizis JC, Madelmont JC & Chollet P (2003) Methionine dependency and cancer treatment. *Cancer Treat Rev* **29**, 489–499.
3 Ali V & Nozaki T (2007) Current therapeutics, their problems, and sulfur-containing-amino-acid metabolism as a novel target against infections by 'amitochondriate' protozoan parasites. *Clin Microbiol Rev* **20**, 164–187.
4 Alexander FW, Sandmeier E, Mehta PK & Christen P (1994) Evolutionary relationships among pyridoxal-5′-phosphate-dependent enzymes. Regio-specific alpha, beta and gamma families. *Eur J Biochem* **219**, 953–960.
5 Tanaka H, Esaki N & Soda K (1985) A versatile bacterial enzyme: L-methionine γ-lyase. *Enzyme Microb Technol* **7**, 530–537.
6 Nakayama T, Esaki N, Sugie K, Beresov TT, Tanaka H & Soda K (1984) Purification of bacterial L-methionine gamma-lyase. *Anal Biochem* **138**, 421–424.
7 Kreis W & Hession C (1973) Isolation and purification of L-methionine-alpha-deamino-gamma-mercaptomethane-lyase (L-methioninase) from *Clostridium sporogenes*. *Cancer Res* **33**, 1862–1865.
8 Faleev NG, Troitskaya MV, Paskonova EA, Saporovskaya MB & Belikov VM (1996) L-methionine-γ-lyase in *Citrobacter intermedius* cells: stereochemical requirements with respect to the thiol structure. *Enzyme Microb Technol* **19**, 590–593.
9 Manukhov IV, Mamaeva DV, Rastorguev SM, Faleev NG, Morozova EA, Demidkina TV & Zavilgelsky GB (2005) A gene encoding L-methionine gamma-lyase is present in *Enterobacteriaceae* family genomes: identification and characterization of *Citrobacter freundii* L-methionine gamma-lyase. *J Bacteriol* **187**, 3889–3893.
10 Dias B & Weimer B (1998) Purification and characterization of L-methionine gamma-lyase from *Brevibacterium linens* BL2. *Appl Environ Microbiol* **64**, 3327–3331.
11 Yoshimura M, Nakano Y, Yamashita Y, Oho T, Saito T & Koga T (2000) Formation of methyl mercaptan from L-methionine by *Porphyromonas gingivalis*. *Infect Immun* **68**, 6912–6916.
12 Lockwood BC & Coombs GH (1991) Purification and characterization of methionine gamma-lyase from *Trichomonas vaginalis*. *Biochem J* **279**, 675–682.
13 Tokoro M, Asai T, Kobayashi S, Takeuchi T & Nozaki T (2003) Identification and characterization of two isoenzymes of methionine gamma-lyase from *Entamoeba*

histolytica: a key enzyme of sulfur-amino acid degradation in an anaerobic parasitic protist that lacks forward and reverse trans-sulfuration pathways. *J Biol Chem* **278**, 42717–42727.

14 Rebeille F, Jabrin S, Bligny R, Loizeau K, Gambonnet B, Van Wilder V, Douce R & Ravanel S (2006) Methionine catabolism in arabidopsis cells is initiated by a gamma-cleavage process and leads to S-methylcysteine and isoleucine syntheses. *Proc Natl Acad Sci USA* **103**, 15687–15692.

15 Nozaki T, Ali V & Tokoro M (2005) Sulfur-containing amino acid metabolism in parasitic protozoa. *Adv Parasitol* **60**, 1–99.

16 Anderson IJ & Loftus BJ (2005) *Entamoeba histolytica*: observations on metabolism based on the genome sequence. *Exp Parasitol* **110**, 173–177.

17 McKie AE, Edlind T, Walker J, Mottram JC & Coombs GH (1998) The primitive protozoon *Trichomonas vaginalis* contains two methionine gamma-lyase genes that encode members of the gamma-family of pyridoxal 5′-phosphate-dependent enzymes. *J Biol Chem* **273**, 5549–5556.

18 WHO/PAHO/UNESCO report. A consultation with experts on amoebiasis. Mexico City, Mexico 28–29 January, 1997. *Epidemiol Bull* 13–14.

19 Stanley SL Jr (2003) Amoebiasis. *Lancet* **361**, 1025–1034.

20 Samarawickrema NA, Brown DM, Upcroft JA, Thammapalerd N & Upcroft P (1997) Involvement of superoxide dismutase and pyruvate:ferredoxin oxidoreductase in mechanisms of metronidazole resistance in *Entamoeba histolytica*. *J Antimicrob Chemother* **40**, 833–840.

21 Wassmann C, Hellberg A, Tannich E & Bruchhaus I (1999) Metronidazole resistance in the protozoan parasite *Entamoeba histolytica* is associated with increased expression of iron-containing superoxide dismutase and peroxiredoxin and decreased expression of ferredoxin 1 and flavin reductase. *J Biol Chem* **274**, 26051–26056.

22 Upcroft P & Upcroft JA (2001) Drug targets and mechanisms of resistance in the anaerobic protozoa. *Clin Microbiol Rev* **14**, 150–164.

23 Dannley RL & Taborsky RG (1957) Synthesis of DL-S-trifluoromethylhomocysteine (trifluoromethylmethionine). *J Organic Chem* **22**, 1275–1276.

24 Zygmunt WA & Tavormina PA (1966) DL-S-Trifluoromethylhomocysteine, a novel inhibitor of microbial growth. *Can J Microbiol* **12**, 143–148.

25 Yoshimura M, Nakano Y & Koga T (2002) L-Methionine-gamma-lyase, as a target to inhibit malodorous bacterial growth by trifluoromethionine. *Biochem Biophys Res Commun* **292**, 964–968.

26 Coombs GH & Mottram JC (2001) Trifluoromethionine, a prodrug designed against methionine gamma-lyase-containing pathogens, has efficacy *in vitro* and *in vivo* against *Trichomonas vaginalis*. *Antimicrob Agents Chemother* **45**, 1743–1745.

27 Inoue H, Inagaki K, Adachi N, Tamura T, Esaki N, Soda K & Tanaka H (2000) Role of tyrosine 114 of L-methionine gamma-lyase from *Pseudomonas putida*. *Biosci Biotechnol Biochem* **64**, 2336–2343.

28 Kudou D, Misaki S, Yamashita M, Tamura T, Takakura T, Yoshioka T, Yagi S, Hoffman RM, Takimoto A & Inagaki K (2007) Structure of the antitumor enzyme L-methionine γ-lyase from *Pseudomonas putida* at 1.8 Å resolution. *J Biochem (Tokyo)* **141**, 535–544.

29 Northrop DB (1999) So what exactly is V/K, anyway? In *Enzymatic Mechanisms* (Frey PA & Northrop DB, eds), Biomed Health Res 250–263.

30 Bakker-Grunwald T, Martin JB & Klein G (1995) Characterization of glycogen and amino acid pool of *Entamoeba histolytica* by 13C-NMR spectroscopy. *J Eukaryot Microbiol* **42**, 346–349.

31 Jakubowski H (2004) Molecular basis of homocysteine toxicity in humans. *Cell Mol Life Sci* **61**, 470–487.

32 Ueland PM & Refsum H (1989) Plasma homocysteine, a risk factor for vascular disease: plasma levels in health, disease, and drug therapy. *J Lab Clin Med* **114**, 473–501.

33 Nozaki T, Tokoro M, Imada M, Saito Y, Abe Y, Shigeta Y & Takeuchi T (2000) Cloning and biochemical characterization of genes encoding two isozymes of cysteine synthase from *Entamoeba dispar*. *Mol Biochem Parasitol* **107**, 129–133.

34 Nozaki T, Asai T, Kobayashi S, Ikegami F, Noji M, Saito K & Takeuchi T (1998) Molecular cloning and characterization of the genes encoding two isoforms of cysteine synthase in the enteric protozoan parasite *Entamoeba histolytica*. *Mol Biochem Parasitol* **97**, 33–44.

35 Gilchrist CA, Houpt E, Trapaidze N, Fei Z, Crasta O, Asgharpour A, Evans C, Martino-Catt S, Baba DJ, Stroup S *et al.* (2006) Impact of intestinal colonization and invasion on the *Entamoeba histolytica* transcriptome. *Mol Biochem Parasitol* **147**, 163–176.

36 Sato D, Yamagata W, Kamei K, Nozaki T & Harada S (2006) Expression, purification and crystallization of L-methionine gamma-lyase 2 from *Entamoeba histolytica*. *Acta Crystallogr F Struct Biol Cryst Commun* **62**, 1034–1036.

37 Nakayama T, Esaki N, Tanaka H & Soda K (1988) Chemical modification of cyseine residues of L-methionine γ-lyase. *Agric Biol Chem* **52**, 177–183.

38 Nakayama T, Esaki N, Tanaka H & Soda K (1988) Specific labeling of the essential cysteine residue of L-methionine gamma-lyase with a cofactor analogue, N-(bromoacetyl)pyridoxamine phosphate. *Biochemistry* **27**, 1587–1591.

39 Goyer A, Collakova E, Shachar-Hill Y & Hanson AD (2007) Functional characterization of a methionine